



Hvammsvirkjun

Geological investigation of Skarðfjall in the South Iceland Seismic Zone

Basement tectonics, Holocene surface
ruptures, leakage, and stratigraphy

Maryam Khodayar¹, Hjalti Franzson¹,
Páll Einarsson², and Sveinbjörn Björnsson³

¹ Íslenskar orkurannsóknir (ÍSOR) Grensásvegur 9, 108 Reykjavík,
Iceland

² Jarðvísindastofnun Háskóla Íslands (Institute of Earth Sciences,
University of Iceland) Sturlugata 7, 107 Reykjavík, Iceland

³ Orkustofnun, Grensásvegur 9, 108 Reykjavík, Iceland

Prepared for Landsvirkjun (The National Power Company) and
Orkustofnun (The National Energy Authority)

ÍSOR-2007/017; LV-2007/065

ICELAND GEOSURVEY

Reykjavík: Orkugardur, Grensásvegur 9, 108 Reykjavík, Iceland - Tel.: 528 1500 - Fax: 528 1699

Akureyri: Rangárvellir, P.O. Box 30, 602 Akureyri, Iceland - Tel.: 528 1500 - Fax: 528 1599

isor@isor.is - www.isor.is

HVAMMSVIRKJUN

Geological investigation of Skarðsfjall in the South Iceland Seismic Zone

Basement tectonics, Holocene surface
ruptures, leakage, and stratigraphy

**Maryam Khodayar¹, Hjalti Franzson¹,
Páll Einarsson², and Sveinbjörn Björnsson³**

¹ Íslenskar orkurannsóknir (ÍSOR) Grensásvegur 9, 108 Reykjavík, Iceland

² Jarðvísindastofnun Háskóla Íslands (Institute of Earth Sciences, University of Iceland) Sturlugata 7, 107 Reykjavík, Iceland

³ Orkustofnun, Grensásvegur 9, 108 Reykjavík, Iceland

Prepared for Landsvirkjun (The National Power Company) and
Orkustofnun (The National Energy Authority)

ÍSOR-2007/017; LV-2007/065

June 2007

ISBN 978-9979-780-61-8

Report no. ÍSOR-2007/017 – LV-2007/065	Date June 2007	Distribution <input checked="" type="checkbox"/> Open <input type="checkbox"/> Closed
Report name / Main and subheadings HVAMMSVIRKJUN Geological investigation of Skarðsfjall in the South Iceland Seismic Zone. Basement tectonics, Holocene surface ruptures, leakage, and stratigraphy		Number of copies 40
		Number of pages 39
Authors Maryam Khodayar, Íslenskar orkurannsóknir Hjalti Franzson, Íslenskar orkurannsóknir Páll Einarsson, Jarðvísindastofnun Háskóla Íslands Sveinbjörn Björnsson, Orkustofnun		Project manager Hjalti Franzson
Classification of report Final report		Project no. 525-012
Prepared for Landsvirkjun (The National Power Company) and Orkustofnun (The National Energy Authority) under the cooperative project “Bergsprungur”		
Cooperators Project carried out in collaboration of ÍSOR, Institute of Earth Sciences and Orkustofnun		
Abstract The planned hydropower projects in Lower-Thjórsá, i.e. Hvammsvirkjun, Holtavirkjun and Urriðafossvirkjun, are located within the South Iceland Seismic Zone, a branch of the mid-Atlantic plate boundary where the relative movement of the lithospheric plates is in the order of 2 cm per year. The construction of hydropower stations and reservoirs in such a highly active seismic zone is a new engineering challenge in Iceland. The geological investigation of the Hvammsvirkjun power plant is the subject of the present study. The power plant is located at the northern boundary of the active seismic zone. The field mapping of the tectonic fractures in this area confirms that the density of recently active fractures decreases northward. The main active fault is a N-S strike-slip fault that cuts through the centre of Skarðsfjall. The fault has also about 25 m throw as seen in stratigraphical units older than the Holocene. This N-S fault was the main source fault of the first earthquake in the major earthquake sequence of South Iceland in 1896. We identify relatively less fractured blocks to the east of this fault as well as to the north of Skarðsfjall and north of the Thjórsá River. If active faults are to be avoided, we recommend that critical structures such as power house, intakes and dams, be built as far to the north and east as possible. Furthermore, we emphasise that the active faults of South Iceland are highly permeable. Therefore, we recommend that reservoir area and depth to be kept to a minimum. We also recommend a survey of geothermal gradients in the entire area of Lower-Thjórsá to interpret leakages and their relation with the active faults.		
Key words Hvammsvirkjun hydropower plant; Skarðsfjall; tectonics; bedrock; Hreppar rift-jump block; South Iceland Seismic Zone; 1896 earthquakes; Holocene surface ruptures; leakage	ISBN-number ISBN 978-9979-780-61-8	
	Project manager's signature	
	Reviewed by Authors, PI	

Table of contents

1. Purpose of the Study	9
2. Geological Framework	9
3. Field Investigations	10
3.1 Stratigraphy	10
3.2 Tectonics	12
3.2.1 Strike and dip of the formations	12
3.2.2 Basement faults	12
3.2.3 Dykes	13
3.2.4 Mineral veins	14
3.2.5 Joints	14
3.2.6 Fault movements in the Holocene	14
3.2.7 Fracture relationships	15
3.2.8 Leakage	16
4. Correlation with the Tectonics of Núpur	17
5. Summary and Interpretation	18
6. Recommendations for Hvammsvirkjun Power Plant	19
7. References	21

List of figures

Fig. 1. Study area with respect to the Hvammsvirkjun hydropower plant projects on Thjórsá River	25
Fig. 2a. Structural map of the Núpur area and correlation with Holocene surface ruptures in the SISZ after Khodayar and Einarsson, 2002	26
Fig. 2b. Geological map of Skarðsfjall after Friðleifsson et al. 1980	26
Fig. 2c. Geological map of Skarðsfjall after Hjartarson and Snorrason, 2001	26
Fig. 3. Synthetic stratigraphical succession of Skarðsfjall	27
Fig. 4. Photo plate of Units 1 to 5	28
Fig. 5. Photo plate of details in Unit 3: Sediments and Tillite	29
Fig. 6. Photo plate of details in Unit 5: Hyaloclastites	30
Fig. 7. Photo plate of Units 5 to 8	31
Fig. 8. Photo plate of Unit 8: Post-glacial formations	32
Fig. 9. Basement Faults	33
Fig. 10. Basement Faults: View on the main N-S fault	34
Fig. 11. Dykes (1)	35
Fig. 12. Dykes (2)	36

Fig. 13. Holocene fault movements (1)	37
Fig. 14. Holocene fault movements (2)	38
Fig. 15. Holocene fault movements (3)	39
Fig. 16. Tectonic structures with potential risks at the site of the planned Hvammsvirkjun power plant	40

List of maps

- Map 1. Geological map of Skarðsfjall: Bedrock and tectonics
- Map 2. Tectonic map of Skarðsfjall: Faults, dykes, Holocene surface ruptures and leakage
- Map 3. Faults and Dykes in Skarðsfjall
- Map 4. Mineral veins in Skraðsfjall
- Map 5. Tectonic joints in Skarðsfjall
- Map 6. Fracture relationships in Skarðsfjall
- Map 7. Faults, dykes, Holocene surface ruptures, and leakage in Skarðsfjall
- Map 8. Correlation between the northerly fractures of Skarðsfjall and the Núpur area

”...Fjallið hristi sig eins og hundur nýkominn af sundi...”

“.... The mountain shook itself like a dog coming from a swim....”

**Thorvaldur Thoroddsen (1899), on the effects of
the 1896 earthquakes in Skarðsfjall**

1. PURPOSE OF THIS STUDY

We undertook the geological investigation of Skarðsfjall in the summer of 2006 as a preparation for the construction of the Hvammsvirkjun hydropower plant by Landsvirkjun (Figs. 1a and b). Skarðsfjall is within the presently active transform zone of South Iceland or the South Iceland Seismic Zone (SISZ). Historical earthquakes as recent as 1896 (Thoroddsen, 1899) have affected Skarðsfjall.

The purpose of our 2006 study was to assess the geological hazards in relation to the construction of the Hvammsvirkjun power plant in the Thjórsá River. To this end, we mapped in detail the stratigraphy and tectonics (Map 1), and analysed faults, fault reactivation during recent earthquakes, dyke injection, mineral veins, tectonic joints, as well as the strike and dip of the formations. We also searched for leakages near the planned construction site. This field investigation is in continuation of our prior studies for Landsvirkjun, which began in 2001 north of Thjórsá River and concerned the construction of the Núpsvirkjun hydro power plant. The present report discusses the detailed study of Skarðsfjall and correlates the data with a few northerly faults north of Thjórsá River around Núpur. The synthesis of all data since 2001 to the north (Núpur to Hagafjall) and the south (Skarðsfjall) of Thjórsá River will be presented separately.

2. GEOLOGICAL FRAMEWORK

Skarðsfjall is located in South Iceland where two structural domains dominate. One is the active South Iceland Seismic Zone (SISZ) connecting the Western Rift Zone (WRZ) to the Eastern Rift Zone (ERZ). Skarðsfjall is presently within this active transform zone. The other is the Hreppar rift-jump block immediately north of the SISZ (Fig. 1a). The Hreppar block is a microplate caught between the propagating ERZ, the receding WRZ, and the SISZ which is itself migrating southward (Einarsson, 1991; Khodayar and Franzson, 2007). The Hreppar block, and the older Borgarfjörður block, constitute the two rift-jump blocks south of 65°N in Iceland.

The stratigraphical succession of Skarðsfjall belongs to the Hreppar formation that spans late Tertiary to Pleistocene and dates from 3.1 m.y. to 0.7 m.y (Aronson and Sæmundsson, 1975; Jóhannesson et al., 1982). The Hreppar formation consists of glacial and interglacial lavas and sedimentary horizons, dating back to uppermost Gauss (Sæmundsson, K., pers. comm., 2007) and lower Matuyama (Friðleifsson et al., 1980; Kristjánsson et al., 1998). Zeolites indicate a paleoburial crustal depth of 500 to 700 m (Sæmundsson, 1970). Acidic rocks are confined to the Stóra-Laxá and Thjórsárdalur central volcanoes. Basaltic sills intruded the Hreppar formation in places and contributed to the build-up of the crust (Khodayar and Einarsson, 2002). Interglacial columnar-jointed lavas younger than 0.7 m.y (Sæmundsson, 1970), and Thjórsá lava with an estimated age of 8.000 y. (Hjartarson, 1988) cover the eroded Hreppar formation. Field observations and borehole data indicate the presence of late glacial sand, tephra, and sediments below the Thjórsá lava (Hjartarson and Snorrason, 2001).

From a tectonic point of view, an anticline could be present midway in the Hreppar microplate, with an axis bending from N-S around Skaftholt and Thjórsárholt to NNE farther north in the Hreppar formation (Friðleifsson et al., 1980). Recent investigations suggest that if the anticline extends as far south as Skaftholt and Thjórsárholt, its axis is likely to be striking NNW (Khodayar and Einarsson, 2002). The latest studies north of the Thjórsá River (Khodayar and Einarsson, 2002; Khodayar and Franzson, 2004; Khodayar and Franzson, 2007), demonstrate that the fracture pattern consists of six sets in the old Hreppar microplate. In addition to the NNE, ENE, and N-S sets (Friðleifsson et al., 1980; Jóhannesson et al., 1982), E-W, WNW, and NNW striking fractures are also present among faults, dykes, mineral veins and joints. Faults belonging to the six sets show both normal and strike-slip motions (Fig. 2a).

Skarðsfjall and surroundings in the SISZ have been mapped a number of times (see e.g. Friðleifsson et al., 1980; Hjartarson and Snorrasson, 2001). The few basement faults and dykes previously mapped in Skarðsfjall itself show northerly and NE striking dip-slip, along with a few WNW striking dykes located mostly in the western part of the mountain (Figs. 2b and c). Holocene surface ruptures have been mapped in the Thjórsá lava surrounding Skarðsfjall (Einarsson et al., 2002). They are considered to be the surface manifestations of underlying N-S striking strike-slip faults. Some of these faults can be correlated with a few older N-S faults in Núpur that have both dip-slips and dextral strike-slips (Khodayar and Einarsson, 2002). However, observations on aerial photographs (Khodayar and Einarsson, 2006) indicate that fracture density in the basement rocks of Skarðsfjall is more than previously mapped. Furthermore, the identification of Holocene surface ruptures has not been previously attempted in Skarðsfjall itself in spite of rather strong effects of the 1896 earthquakes there, as described by Thoroddsen (1899).

3. FIELD INVESTIGATIONS

In 2006, we mapped the bedrock, the strike and dip of the units, 59 basement faults, and 173 dykes (Maps 2 and 3). We recorded 386 mineral veins (Map 4) and 1229 tectonic joints (Map 5), and for the first time found and mapped 51 fractures indicating recent faulting, mostly within Skarðsfjall but also surrounding the mountain (Map 2). Our structural analysis consisted of the strike and dip of all fracture types, sense and magnitude of fault displacements, as well as the thickness and nature of dykes and mineral veins. For overview, we correlate the faults mapped in our study with the fractures mapped by Einarsson et al. (2002) in Thjórsá lavas west and north of Skarðsfjall. The relationship between different fracture types was also investigated (Map 6). Finally, we mapped carefully relevant springs, wetland, and streams with the GPS to check if their location coincides with any fracture trace (Map 7). Results of our stratigraphy and tectonic investigations are presented below.

3.1. Stratigraphy

We grouped the stratigraphical succession into 8 units (Map 1 and Fig. 3) based on change of rock type, erosional contact and discordance. From the oldest to the youngest, the 8 units are:

Unit 1 is found in the southern half of Skarðsfjall and is maximum 250 m thick in the outcrop. The lavas are generally tholeiite with columnar joints (Fig. 4a). About 30 m massive tholeiite lava flows crop out at the base of the series, succeeded by 25 m of tillite. The tillite is a heterogeneous conglomerate with a grayish matrix at the base but becomes finer-grained with yellowish matrix at the top. Some 15 to 16 lava flows, maximum 80 m thick, overly the tillite. In a poor outcrop on the eastern side of the mountain ≥ 1 m tuffaceous sediments intercalate locally the lavas. Six transitional basaltic flows (tholeiite/olivine tholeiite), 25 to 37 m thick, separate these lavas from the uppermost tholeiite flows. These lavas are 5 to 10 m thick and massive, except east of Hvammur where some of the flows show scoriaceous top. The total thickness of the uppermost tholeiite lavas is 50 to 80 m. These are massive flows, on average 10 m thick, and pink to grey-blue at the surface. They are generally coarse-grained, some contain flow lineations and small vesicles that are occasionally filled with zeolites.

Unit 2 is 27 to 45 m thick (Fig. 4a), and consists of two plagioclase porphyritic lavas with maximum 15 m thickness separated by 7 to 15 m coarse-grained olivine tholeiite. Both the olivine tholeiite and the upper porphyritic lavas appear to be thinner towards north.

Unit 3 consists of tillite and fluvio-glacial sediments with a maximum of 150 m (Figs. 4a and 4b). Generally, the tillite crop out at the lower part of Unit 3, and the sediments in the middle and the upper parts have a fluvio-glacial character (Fig. 5a). The basal tillite is 30 m thick, with heterogeneous rounded elements, up to 15 cm long, alternating with blue/brown silts. Some 35-40 m of fine silts succeed the tillite and contain sedimentary figures resulting from past water currents. Most of Unit 3 (70-80 m thick) consists of alternating fine compact silts and massive grey tillite. The tillite is of finer size with both angular and rounded heterogeneous elements. Few thin fine- to coarse-grained olivine tholeiite sills intrude the silts. Generally, Unit 3 is thinner (50-70 m) in the western half of Skarðsfjall.

Unit 4, or the series of Miðfell, is very likely a part of Unit 3. The series is maximum 120 m thick and consists of olivine tholeiite, tillite, and sediments (Figs. 3, 4b, and Map 1). At least 3 layers of olivine tholeiites with a total thickness of 20 m crop out at the base. These olivine tholeiites are only to be found to the south and west of Miðfell. The lowest olivine tholeiite is slightly porphyritic and contains small pyroxenes. About 50 m massive tillite, with centimetre-scale heterogeneous sub-angular elements in a bluish matrix (Fig. 5b) covers the olivine tholeiite. The succession above the tillite contains 20 m tholeiite succeeded by a 15-m fluvial sediments. This succession is in turn overlain by a series of maximum 40 m thick olivine tholeiite flows. These olivine tholeiites are thick in Miðfell but thinner towards the north and die out east of Hvammur in the uppermost sediments of Unit 3 (Map 1). Hjartarson and Snorrason (2001), and Kristinsson (2004) interpret the olivine tholeiite layers as sills intruding the hyaloclastites. However, no field evidence was found to attribute the series of Miðfell to an intrusion. Therefore, we interpret these olivine tholeiite rocks as lavas that flowed locally into the tillite/sediments of Unit 3 and not as an intrusion into this unit. The tectonic aspect of these olivine tholeiite flows is discussed below.

Unit 5 consists of hyaloclastites of olivine tholeiite composition, with a maximum thickness of ≥ 135 m. The hyaloclastites are a product of a single sub-glacial eruption. They form a lenticular mountain with sub-horizontal layers of pillow basalt/breccias in the central part and steeply-dipping layers (foreset bedding) towards the margins (Fig. 6a). Steeply-dipping layers are well visible to the north of the mountain and indicate the rapid thinning of the hyaloclastite formation. Their absence south of the mountain indicates that the formation has been eroded away there (Map 1). The lower and middle parts of the hyaloclastite formation consist of breccia, tuffs, and pillow lavas (Figs. 6b and c), as well as a conspicuous network of dykes and sills. The dykes are described and interpreted in the chapter on tectonics, below. The upper part of the formation consists more dominantly of finer-grained breccias and tuffs in yellow matrix (Fig. 6d). Occasionally, fragments of lacustrine sediments appear in the uppermost layers to the north and the south of the hyaloclastite mountain. Conspicuous pillow lavas are rare and sparse in the uppermost layers.

Unit 6 banks up against the northern slopes of the hyaloclastite mountain. At the surface, the contact of this unit and Unit 5 appears only north of Skarðsfjall where the main N-S fault plays the contact between the two units (Fig. 7a). The absence of dykes in Unit 6 indicates that this unit is younger than Units 1 to 5. The total thickness of Unit 6 is roughly 150 m and it consists of three formations. More than 15 m thick tholeiite lavas crops out at the base, succeeded by 5 to 10 m tuff-rich fluvio-glacial sediments with heterogeneous fragments up to 20 cm in size. A plagioclase-porphyritic lava flow overlies the sediments, followed by flaky columnar jointed olivine tholeiite lava. With a total thickness of 100 m, some 26 porphyritic lava flows, each 2 to 8 m thick, overly the olivine tholeiite. As these porphyritic lavas are faulted, their real thickness cannot be estimated. However, the maximum vertical fault displacement in Skarðsfjall is on average 13 m. Therefore, the few faults in the porphyritic lavas would not substantially alter the total thickness of the series. The porphyritic lavas are of pahoehoe type and without intercalated sediments, indicating a possible monogenic lava shield.

Units 1 to 6 are of lower Matuyama age and they belong to the oldest formations found in South Iceland. Contrary to the series north of Thjórsá River (Khodayar and Einarsson, 2002; Khodayar and Franzson, 2004), relatively few sills intrudes the Hreppar formation in Skarðsfjall.

Unit 7 or the interglacial columnar-jointed lavas is found to the northeast of Skarðsfjall. Its thickness is 15 m and it belongs to the normally magnetised basaltic flows of Brunhes geomagnetic epoch (Map 1 and Fig. 7b). This unit lies unconformably on top of the basal tholeiite lavas of Unit 6 with a possible erosional contact and a discordance. Interglacial lavas present only medium-sized columnar joints, and the two-tiered facies with the upper brecciated part, visible north of Thjórsá River (Khodayar and Einarsson, 2002), is absent here.

Unit 8 is divided into four different formations (Fig. 3). The oldest is the 8.000 y. old plagioclase-porphyrific Thjórsá lavas (Hjartarson, 1988). These lavas are 15 m thick and they cover much of the lowland around Skarðsfjall. Eolian sediments cover Thjórsá lavas and the older units in places (Map 1). Only to the east of Hvammur eolian sediments do cover locally older fluvial sediments (Fig. 8a). The fluvial sediments are 2-3 m thick, and they consist of alternating rounded heterogeneous medium and finer size gravel in a grey sandy matrix. The sediments are likely to be remnant of a river bed along the northerly valley within Skarðsfjall. Eolian sediments are 1 to 10 m thick, and they are thickest north of Skarðsfjall (Figs. 8b and c). They consist of brownish/yellowish tuff and clay, and are dominantly made of Hekla tephra layers (Fig. 8d). The youngest group of Unit 8 is the Holocene soil and sand (superficial formation), covering mostly the low-land around Skarðsfjall.

3.2. Tectonics

The “N” value on rose diagrams of Maps 3 to 6 indicates the total number of measurement, and “Max.” values the number of measured fractures along the most frequent strike.

Note that we describe the strikes of the fractures from N0° to 90°W and from N0° to 90°E. Such a description is also consistent with N-S, NNW, WNW, etc. designations of fracture trends.

3.2.1. Strike and dip of the formations. Units 1 to 6 strike on average N80°W, and dip 7°-10° NE (Map 1), similar to the series that extend from Núpur eastwards north of Thjórsá River (Khodayar and Einarsson, 2002). However, dip values could be as shallow as 4° and high as 12° locally in Skarðsfjall. The dip of the interglacial lavas (Unit 7) is difficult to measure in the field, but it is assumed that their shallow dip is in the range of 2° to 3°, similar to other localities north and west of Skarðsfjall. Interglacial lavas are discordant on the older tholeiite lavas of Unit 6. Post-glacial formations of Unit 8 do not present a regional tectonic tilt. They are assumed to have only tilt of depositional nature.

3.2.2. Basement faults cut through units older than Unit 8 (Map 1). The faults strike dominantly northerly (N10°W-N20°E) with a peak at N10°E-N20°E, then NNE (N30°-N40°E), ENE (N50°E-N60°E), and WNW (N70°W-N80°W) (Map 3a). The northerly and the ENE faults are respectively parallel to the main and the conjugate Holocene surface ruptures in the SISZ (Map 2), while the NNE faults are rift-parallel. Our fracture analysis north of Thjórsá River suggests that all the four sets can form within a transform zone similar to the SISZ (Khodayar and Franzson, 2007). Faults dip steeply in Skarðsfjall, between 80° and 90°. No preferential dip direction is associated with any of the fault sets. Horsts and grabens are present along various fault strikes (Map 2 and Fig. 9a). More major faults than mapped could exist both in the hyaloclastites of Unit 5 (Fig. 9b) and in the porphyritic lavas of Unit 6. However, the fault types and their magnitude of displacements could not be determined as the faults crop out in homogenous host rocks. All identified fault sets show normal-slip (Map 3a), but due to the lack of marker horizon, horizontal offsets resulting from strike-slip could not be identified. The magnitude of vertical displacement (throw) across marker horizons could be estimated only for 24 faults in Units 1 to 6. These throws range from 3 to 25 m, with the exception of one northerly fault showing 35 m throw. About 1/3 of the faults have throws exceeding 10 m, and generally the largest throws are along northerly and WNW faults. The

maximum thickness of fault breccia along basement faults is 5 m. The breccia was observed above Hvammur, at the intersection of an ENE fault and a N-S fault into which a northerly dyke is possibly injected. Fault traces are eroded and covered with grass, making the observation of deformation on the fault planes difficult.

At least two of the basement faults are of major tectonic importance. One is the main N-S fault, and the other is a northerly fault in the eastern part of the mountain. The main N-S fault strikes N180°E, has about 3.5 km visible length, and dissects Skarðsfjall longitudinally (Maps 1 and 2). North of Skarðsfjall, the fault separates the hyaloclastites from the tholeiite/olivine tholeiite of Unit 6 (Map 1 and Fig. 10a). In the middle part of the mountain, a valley exists on the fault trace cutting through the hyaloclastites (Fig. 10b). The vertical fault displacement (throw) cannot be estimated, neither to the north nor in the middle part of the mountain. But to the south, the throw of the N-S fault is 25 m down to the east based on the displacement of the lavas in Units 1 and 2 (Fig. 10c). The N-S fault could be younger than the sediments/tillite of Unit 3. However, south of Miðfell, field data suggest that the fault may have been active earlier (Map 1). The sediments/tillite (Unit 3) covers the olivine tholeiite lavas (Unit 4) to the west of the N-S fault and the porphyritic lavas (Unit 2) east of it. Likely, the olivine tholeiite lavas have flowed from the west. Had the N-S fault been westward dipping, then these would have banked against the fault scarp, accumulating on top of the underlying block tilted by the N-S fault. But that is not the case as the fault is eastward dipping (Map 1). Therefore, the olivine tholeiite lavas are likely to have thinned out rapidly towards the east and disappeared before reaching the fault scarp.

The other important northerly fault in the eastern part of Skarðsfjall strikes N12°E, has around 2 km visible length, and crops out mainly in the hyaloclastites in its northern part (Map 1). In its southern portion, the fault displaces Units 1 to 3 vertically by 15 m down to the west. Present-day microearthquake activity in Skarðsfjall appears to be associated with the main N-S fault and this northerly fault.

3.2.3. Dykes fall into two sets in our detailed mapping (Map 3b). The map of Hjartarson and Snorrason, (2001) does not reflect these two sets as only few of the dykes, mainly located west of the main N-S fault and mostly WNW striking, were mapped by those authors. In our mapping, one of the two sets strikes dominantly northerly (N10°W-N00° and N10°E-N20°E), and secondarily ENE (N50°E-N60°E), parallel to the most common basement faults and to the recently active faults in the SISZ (Maps 3a and b). The other set consists of WNW and NNW dykes with their distribution peaks at respectively N60°W-N70°W and N20°W-N30°W. Though NNE rift-parallel dykes are very few, they are among the longest dykes. All dykes are olivine tholeiite, similar to the pillow basalts in the hyaloclastites, and they present four facies: (a) bluish vesicular; (b) black coarse-grained very vesicular; (c) fine-grained aphyric; and (d) fine-grained with small-size olivine, plagioclase, or pyroxene phenocrysts. Often 1 to 5 cm black chilled margin is associated with dykes' edges. Dyke thickness ranges from 0.2 to 2.4 m, and the thickest dykes are in the northern slope of Skarðsfjall (Fig. 11a).

In order to better understand their significance, we plotted the dykes separately on a map, added the contour of the hyaloclastites (Map 3b), and analysed the dyke distribution. Most dykes are concentrated in the lower and the middle parts of the hyaloclastites. There, their edges are pillow-like (Figs. 11a and b), they turn into sills and breccias, and they die out in the upper part of Unit 5. A few N-S and NW dykes were mapped outside of the hyaloclastite formation in the older Units 1 to 4 (Maps 1 and 3b; Figs. 11c and d). The presence of a few dykes in units older than the hyaloclastites indicates that at least some of the dykes reach deep into the crust and are not restricted to the hyaloclastite formation. We interpret the dykes as feeder dykes based on: (a) WNW dykes are mostly concentrated west of the main N-S fault (Figs. 12a and b), while segments of the same dykes strike NW and NNW east of this fault, evoking "ring dykes" (Figs. 12c and d). The bend in the strikes of the dykes occurs around a centre from which the hyaloclastites erupted through dykes (Map 3a). This centre is located on the trace of the main N-S fault and at the intersection of an ENE fault (Map 3b). The "non ring dykes", however, are dominated by the northerly and ENE dykes (Map 3b). (b) Most WNW and NW dykes around the eruptive

centre are highly vesicular, with vesicles parallel to the dykes' edges even in case of multiple dyke injection, indicating their eruptive character.

3.2.4. Mineral veins were measured in various locations and formations (Maps 4a and b). Map 4a shows the distribution of the measured veins and the location of major fractures. Mineral veins strike dominantly N50°E-N60°E, parallel to the conjugate fractures in the SISZ. Vein thickness in Skarðsfjall is from 1 to 3 mm, exceptionally 5 mm, with only two veins of 10 cm thickness located in the fault zone of a NNE fault. The infilling of veins is mostly opal and zeolites. The three rose diagrams on Map 4b show our attempt to spot changes in the strike of the veins with respect to the relative age of the host rock. Veins in Unit 2 were measured only in one place, i.e. above Hvammur. The dominant strike of the veins is NW (N20°W-N40°W), similar to the adjacent NW dykes. Therefore, these veins are not representative of Unit 2. Most veins were measured in the sediments/tillite of Unit 3 and strike dominantly ENE. Measured veins in Unit 5 show a slight rotation and they strike NNE (N30°E-N40°E), parallel to the rift when the hyaloclastites erupted from rift zone. However, a plausible conclusion cannot be presented due to the low number of measured veins. A greater number of veins at more locations in Skarðsfjall is needed to reach conclusive results.

3.2.5. Joints were measured in greater number, in more locations, and in four different rock units in Skarðsfjall (Maps 5a and b). Generally, joints strike dominantly northerly (N10°E-N20°E). Joints of this set are often tightly spaced in deformation zones of faults and dykes. Map 5b shows our attempt to spot changes in the dominant strikes of joints by comparing measurements in Units 1, 2, 3, and in eolian sediments of Unit 8. Joints strike dominantly northerly (N10°E-N20°E) in the tillite/sediments of Unit 1, in the olivine tholeiite of Unit 2, and in tillite/sediments of Unit 5. However, the strikes of the joints in eolian sediments differ slightly from the strikes of joints in older units. Joints strike dominantly northerly with a peak at N20°E in eolian sediments, especially adjacent to northerly faults. However, the strike range of joints is wider (N10°W-N20°E) in eolian sediments northeast of Skarðsfjall. There, two additional sets are prominent, striking NNE (N30°E-N40°E) and WNW (N60°W-N70°W), but the strikes of the three sets are blurred though (Map 5b).

3.2.6. Fault movements in the Holocene. In his description of the 1896 earthquakes and their effects on Skarðsfjall, Thorvaldur Thoroddsen states (1899): "...*The mountain shook itself like a dog coming from a swim...*". This statement is confirmed by our mapping for the first time of Recent active faults in Skarðsfjall (Maps 2 and 3a). We found and mapped 51 structures of variable lengths showing evidence of recent movements. Of these, 8 structures do not show any relation with underlying basement fractures, but 43 structures are along older basement faults and a few non ring dykes. Thus all but 15 of the mapped basements faults show signs of ruptures during the Holocene. Arrays of recent faulting were observed in all units. Lava structures in Thjórsá lavas could in some cases be mistaken as surface ruptures resulting from fault movements because of a similar outlook. Therefore, we mapped the surface ruptures in Thjórsá lavas only when we were reasonably confident they are of tectonic origin. This resulted in a lower number of active faults in Thjórsá lavas than are possibly present. The most important features of the mapped Holocene surface ruptures are:

- Segments of recently active faults strike dominantly northerly (N10°E-N20°E), similar to the basement faults and to the non-ring dykes, then NNE (N30°E-N40°E), and ENE (N50°E-N60°E). To a lesser degree, these segments strike E-W (N80°E-N90°E), and WNW (N60°W-N70°W) (Map 3). Fracture arrays present an *en échelon* arrangement at any scale (Figs. 13a-c, 14a-e, 15a-g). They are left-stepping in case of dextral and right-stepping in case of sinistral strike-slips movements. On this ground, northerly to NE fractures (N10°W-N40°E) are dextral and NE-ENE to WNW fractures (N40°E-N90°E and N80°W-N90°W) sinistral (Map 3a). However, in rare cases, opposite movements were also observed along the NE (N40°E), i.e. sinistral, and the WNW (N80°W), i.e. dextral strike-slip faults. Arrays of recently active faults appear in different landscapes (Figs. 13 to 15) ranging from flat land at the bottom of the

slopes and in the central valley on top of Skarðsfjall, to the slopes themselves where in few cases the sense of motion could not be deduced due to lack of clear *en échelon* organisation.

- Individual segments of recently active faults consist mostly of sink holes and sometimes of a few push-ups. The length of individual segments ranges from a few metres to hundreds of metres. The longest segment is 450 m, and it is located in the central-southern part of the main N-S fault (Map 3a). Individual sink holes vary in length and width from less than a metre (Fig. 13c) to several metres (Fig. 15), while push-ups are generally less than half-a-metre except on the main N-S fault where they reach several metres in diameter and height (Fig. 13a and 14a). The main N-S fault shows most evidence of recent ruptures in 7 places along its trace, varying from a couple of sink holes to tens of holes and the biggest push-ups (Map 3a; Figs. 13 and 14).
- The Holocene surface ruptures indicate both strike- and dip-slips. The magnitude of horizontal offset could not be estimated for strike-slips due to the lack of markers in the field, but vertical displacements (throws) are indicative of cumulative dip-slips. The maximum throw along recently active faults during single earthquake is 0.5 m (Figs. 13b and 15g). However, some arrays of recently active fault are within prominent grabens that have stepped fault scarps up to 2.5 m height (i.e., Figs. 15b and f). These grabens strike N-S (West of Skarðsfjall), E-W (central part of Skarðsfjall), and WNW (Southwest of Skarðsfjall) (Map 3a). Some of these grabens themselves are on the traces of basement faults that show throw up to tens of metres in the older units. The best example of cumulative throw is the main N-S fault. The throw in the southern part of this fault is 25 m in Units 1 and 2 (Fig.10c), but 0.5 m in Holocene soil (Fig. 13b). The comparison between the fault throws in the older and the younger stratigraphical units suggests that throw could accumulate with time along single faults with each earthquake.

The density of Holocene surface ruptures decreases drastically in the “NE block” of Skarðsfjall (Map 2). This block is limited to the south by an E-W line coinciding roughly with an E-W recently active fault in eolian sediments on top of interglacial lava (Map 1). This E-W boundary could also be interpreted as a boundary between the structurally weak hyaloclastites and the compact interglacial lavas, but the lavas and hyaloclastites are too thin to influence the location of a seismic fault that cuts through several kilometres of crust. To its west, the “NE block” is bounded by the main N-S fault that plays also as the contact between Units 5 and 6. Holocene surface ruptures were rarely found in the porphyritic lavas of Unit 6, but they could be more numerous because identifying them in homogeneous hard rock is more difficult. However, no Holocene surface ruptures were found north of the E-W boundary in eolian sediments, indicating that a big portion of the “NE block” has not been fractured during the Holocene. This observation is also supported by the low frequency of northerly joints in eolian sediments cropping out in the “NE block” (Maps 5a and b).

3.2.7. Fracture relationships. A comparison between the strikes of all fracture types indicates that the non-ring dykes, the faults, and the joints have a similar dominant strike, e.g. northerly, parallel to the main active faults in the SISZ (Map 6a). Joints are in deformation zones of faults and dykes, but mostly associated with faults. Mineral veins are as much associated with faults as with dykes. They strike, however, dominantly ENE, e.g. parallel to the conjugate fractures in the SISZ. A similar discrepancy between the strikes of mineral veins and the other fracture types was also observed in the series north of Thjórsá River (Khodayar and Einarsson, 2002; Khodayar and Franzson, 2004).

Cross-cutting relations between different fracture types are not conclusive, but cross-cutting dykes indicate that all fracture sets opened at the same time and were injected by the same olivine tholeiite magma during a single event. Although most dykes are in Unit 5 and feeder of the hyaloclastites, they show a strong relation with older basement faults. Our detailed fracture map shows that at least a few northerly and ENE dykes and two NNE dykes are injected into faults

(Map 6b). It is assumed that some of these faults may have been concomitant or older than the hyaloclastites and were filled by magma when the dykes fed the hyaloclastites (Map 6c).

As to the Holocene fault movements, arrays of Holocene surface ruptures were mapped along the majority of basement faults and of a few non-ring dykes (Map 6b). Recent movements are along six fracture sets, all inherited from the basement. Some of our mapped basement faults and Holocene surface ruptures to the west and north of Skarðsfjall are in the continuation of fractures mapped by Einarsson et al. (2002) (Map 6b).

3.2.8. Leakage. Skarðsfjall and surroundings are rather dry areas with very few springs and streams at the surface. Exploratory drilling north of Skarðsfjall has found the ground water level at 99-100 m.a.s.l or 6-7 m depth (Snorrason, S.P., pers. comm., 2007). There are, however, several past and present water sources found in the region. Some of these might represent hanging water tables of recent precipitation, other might be leakages on fractures driven by the waterhead of precipitation on the mountain. Therefore, we paid a special attention to the location of water sources in order to check if any relation appears with tectonic fractures. We observed three types of water sources: (a) wetland, (b) streams, (c) ponds and springs, and mapped them with the GPS with a resolution of 1-2 m as to their exact location. All three types are on tectonic fractures striking dominantly northerly and ENE, but also E-W and WNW (Map 7a). We, therefore, suspect these to be leakages on fractures rather than arbitrary distributed hanging water tables.

The most prominent wetland is to the north of Skarðsfjall in a depression of 300 m x 40 m, caught between the northern slope of the hyaloclastite mountain and a network of northerly dykes (Map 7a). Stagnant shallow water appears occasionally in this iron-rich swampy depression. The southern part of the wetland coincides with the trace of an ENE fault that has possibly shaped the slope of the hyaloclastites. Two segments of recently active fractures and an ENE dyke appear on this fault trace. We interpret this wetland as tectonically controlled.

Streams appear to the north, northeast, and west-southwest of Skarðsfjall (Map 7a). Water flows out of the rocks at the same relative height within each of these areas independently of the rock type. To the northeast, the two most prominent streams appear in hyaloclastites and are located on two northerly dyke and fault with evidence of dextral movements during the 1896 earthquakes. Another prominent stream, which was frozen at the time of the mapping late during the field season, appears in Unit 6 on a major undifferentiated NE striking fault in porphyritic lavas. South of Hvammur at least five streams appear at the same height and flow down the slopes to the west of Skarðsfjall. All these streams originate in basement faults that were activated during the 1896 earthquakes. East of Hvammur, however, a stream dried out after the earthquakes. Similarly, north of Hvammur, two springs lie near an ENE dip-slip fault. These springs supplied the farmers for local uses in the past, but they are presently dry. It is unknown whether their drying up was caused by earthquakes.

Several springs and ponds are at the surface of Skarðsfjall and surrounding the mountain. The most important of these springs are to the northwest and the north of the mountain (Map 7a). Northwest of Skarðsfjall there are two series of cold springs and dried ponds immediately north of Thjórsá River. Algae, iron-rich mud, or swamp is associated with many of the springs and ponds. At the time of the mapping, the air temperature was 2.4°C, while the temperature of water in the springs ranged from 2.4°C to 8°C. The two series of springs are each aligned northerly on the traces of two faults that are spaced roughly 380 m and stretch south of the Thjórsá River. The westernmost fault is in Thjórsá lava and it is in the continuation of a prominent northerly dextral strike-slip fracture array mapped by Einarsson et al. (2002). The easternmost northerly fault is also dextral strike-slip in Thjórsá lava, but stretches through the hyaloclastites and displaces vertically the porphyritic lavas of Unit 2 by at least 10 m to the west. Both these northerly faults lie under the planned Hvammsvirkjun power plant. The manifestations north of Skarðsfjall are all located south of Thjórsá River, in Holocene soil above the porphyritic lavas of Unit 6 (Map 7a). The springs and ponds are immediately east of the main N-S fault surrounded by extremely dry

land. The springs are about 6°C in temperature and similarly, algae, green moss, iron-rich mud or swamp are associated with many of them (Maps 7b to f). The GPS mapping of these manifestations shows that most of the springs are on a possible ENE Holocene fault, and a few on a northerly Holocene fault (Map 7a). No evidence of recent displacement was found along the northerly and ENE faults, though the fault traces are well visible both on aerial photograph and in the topography in the porphyritic lavas of Unit 6.

Finally, some sinkholes associated with recent surface ruptures are filled with water and algae, green moss, iron-rich swamp are occasionally associated. These manifestations were observed locally along five Holocene faults in the hyaloclastites, all located to the east of the main N-S fault (Map 7a). Two of these faults strike E-W, one is a sinistral Holocene surface rupture south of the “NE block” (Fig15e), and the other is a dip-slip fault at the southern tip of the hyaloclastite mountain with 7 m throw to the north. The third one is a major northerly fault, which has 15 m throw to the west in the basement rock and shows evidence of dextral strike-slip movement during the 1896 earthquakes. The fourth and fifth faults strike ENE and are located in the middle of the mountain. They show evidence of sinistral slip movements during the 1896 earthquakes. No leakage was observed along the main N-S fault.

4. CORRELATION WITH THE TECTONICS OF NÚPUR

Map 8 shows both the structures mapped in Skarðsfjall in 2006 as well as the northerly faults mapped in the Núpur area (Khodayar and Einarsson, 2002). The purpose of this compilation is firstly to check whether there is a change in the tectonic style between the north and south of Thjórsá river, and secondly how the faults on both sides of the river match together. A general geological synthesis is in preparation and will discuss data from both sides of the river including all the faults and dykes of Núpur area.

The general strike of the formations older than interglacial lavas is on average N100°E on both sides of the river with a general dip of 5°-10° to the NE (Map 8). Dips as high as 15° were observed in Núpur area, and are likely caused by local tilt of blocks across faults (Khodayar and Einarsson, 2002). Despite the volcanic material originated in a rift zone, the crust in Skarðsfjall does not strike NNE, i.e. parallel to the rift axis.

As Map 8 shows, the density of basement fractures is higher in Skarðsfjall than in the Hreppar formation north of Thjórsá River. This higher fracture density could be only local. However, the density of recently active fractures is much higher south of Thjórsá river than north of it, indicating that most of the earthquakes in the Holocene occur south of the river.

At least three northerly faults mapped on each side of Thjórsá River match perfectly together.

- The westernmost fault is in Stóri-Núpur, it strikes N-S and has both dip- and strike-slips. The fault throw is 10 m to the west in Hreppar formation and the sense of slip is dextral based on near-horizontal striae on the fault plane (Khodayar and Einarsson, 2002). Three segments of recently active faults appear in Thjórsá lava on the trace of this fault to the south of the river (Einarsson et al., 2002). The three segments are also aligned N-S and are dextral (Map 8).
- The two other northerly faults are on both sides of Viðey island. The westernmost fault stretches from Miðfell to the north all the way south of Thjórsá River and very likely connects to the major northerly dextral Holocene fault in Thjórsá lava. North of Thjórsá River, the fault shows dip-slip with a throw ≥ 15 m down to the east (Khodayar and Einarsson, 2002). In 2006, we found, adjacent to the river, leakage along this fault (Map 7). The easternmost fault is farther east of Viðey island in the Hreppar block and is an undifferentiated fault (Khodayar and Einarsson, 2002). South of the river, this fault shows both dip-slip with a throw to the west, and

dextral strike-slip based on a few left-stepping *en échelon* arrays of surface ruptures on the fault trace (Maps 7 and 8). Leakage was also mapped along this fault adjacent to the river.

5. SUMMARY AND INTERPRETATION

We mapped in detail the tectonics and stratigraphy of Skarðsfjall to assess the hazards in relation to active faults and leakages at the site of the planned Hvammsvirkjun power plant in the Thjórsá River. Fractures show signs of activity through time as evidenced by their frequency, spatial relationships, magnitude of displacements, and recent activity. Below is the summary of our main tectonic results.

1. Fractures may be classified into six sets according to strike, dominantly northerly and ENE parallel to the conjugate set of recently active faults in the SISZ, but also E-W, WNW, NNE, and to a lesser degree NNW.
2. Basement faults are numerous in units 1 to 5, but fewer in units 6 and younger. Faults strike dominantly northerly and ENE, then E-W, WNW, and NNE. The horizontal offset for strike-slips could not be determined along basement faults due to lack of markers, but basement faults have an average vertical displacement (throw) of 13 m, ranging from 3 to 35 m. The highest throws are along northerly faults. The two most prominent basement faults strike N-S and N12°E, with respectively 3.5 km and 2 km visible lengths, and 25 m and 15 m throws. The longer of the two faults dissects Skarðsfjall longitudinally, and the other cuts the hyaloclastites in the eastern part of Skarðsfjall.
3. Dykes are organised in two sets, one striking dominantly northerly and to a lesser degree ENE, and the other WNW and NNW (the ring dykes). All dykes are olivine tholeiite similar to the hyaloclastites of Unit 5. They have pillow-like edges and are a part of the hyaloclastites while a few cut older units. No dyke was seen in Units 6 and younger. The density of the dykes and their bend from WNW to NNW in the central part of Skarðsfjall suggest that the hyaloclastites originated at an eruptive centre located on the main N-S fault and at the intersection with an ENE fault. Eruptive dykes fed the hyaloclastites from this centre and injected into the fractures parallel to the centre (ring dykes) as well as also into older northerly and ENE faults parallel to the conjugate set of earthquake fractures in the SISZ.
4. Fracture relationships indicate that faults, dykes, and tectonic joints strike dominantly northerly, but mineral veins strike ENE. Veins are associated with both dykes and faults, but joints rather with faults.
5. Most basement faults and portions of dykes show signs of activity during the Holocene. These fractures strike along six sets, but dominantly northerly, ENE, and E-W. Active faults with northerly to NE strikes are dextral, and ENE to E-W striking faults are sinistral. The magnitude of horizontal offset could not be estimated along the fractures, but their throws are between 0.5 and 2.5 m.
6. The majority of Holocene surface ruptures occurs on older basement faults. A comparison between the fault throw in the older and the younger stratigraphical units indicates that throw accumulates along single fault planes. The best example is provided by the main N-S fault, which has 25 m throw in Units 1 and 2 but only 0.5 m during a single earthquake in 1896.

7. The main N-S fault cutting through Skarðsfjall shows abundant evidence of Holocene movements in 7 places along its trace. Individual segments range from a couple of sink holes over 2-3 m length to tens of holes and a few metres-scale push-ups over 450 m length. Due to the frequency and freshness of these manifestations we suggest that the first mainshock of the 1896 earthquake sequence originated on this fault. This is further supported by present-day microearthquake activity, which indicates that this N-S fault and the northerly fault in the eastern part of Skarðsfjall are still active.

8. The “NE block” in Skarðsfjall is presently bounded by the main N-S fault and a recently active E-W fault, respectively located to its west and south. This tectonic configuration could date already from Matuyama when the block subsided along these two faults and was filled with porphyritic lavas of Unit 6, which are present only in this part of Skarðsfjall. The block still appears as tectonically different during Holocene. The density of recently active fractures decreases in this block with no fractures north of the E-W boundary fault in at least the eolian sediments. Furthermore, the frequency of northerly joints is low in eolian sediments indicating that a big portion of the “NE block” has not been fractured for a long time.

9. Wet land, streams, cold springs, and ponds appear on fractures striking dominantly northerly and ENE, but also E-W and WNW. No leakage was observed on the main N-S fault, but on other fractures relevant to the power plant. To the northwest of Skarðsfjall, leakage appears on two northerly dextral strike-slip faults inherited from basement. Both faults stretch from the Hreppar block southward and cross the planned site of Hvammsvirkjun power plant. Immediately east of the main N-S fault leakage appears on a northerly and ENE conjugate fracture set that is located very near the site of the power plant.

Although the geological series of Skarðsfjall were generated in a rift zone, NNE-NE rift-parallel structures are not frequent. Instead, the stress field of the transform zone has had the greatest influence since early history of Skarðsfjall and resulted in a conjugate set of northerly and ENE fractures. Evidence of this early influence of the transform zone was also found in seismic disturbances of then unconsolidated Matuyama sediments near Thjórsárholt (Khodayar and Einarsson, 2002). The fracture pattern of Skarðsfjall is dense compared to that of the Hreppar block to the north. To the south of the river, basement fractures were intensively reactivated during the Holocene, e.g. during the 1896 earthquakes. The transform fault regime is still dominant, causing seismicity and leakage along the same dominant fracture sets as in the old basement. Most evidence of these manifestations is seen in the median valley and the northern part of Skarðsfjall (Fig. 16).

6. RECOMMENDATIONS FOR HVAMMSVIRKJUN POWER PLANT

Our detailed mapping of stratigraphy and tectonics, as well as the structural analysis of 67 faults, 173 dykes, 1229 tectonic joints, and 386 mineral veins in Skarðsfjall indicate that major fractures have been active through time, up to the present. Therefore, careful considerations must be given to active faults and leakages should the Hvammsvirkjun power plant be built as planned.

In Fig. 16 we plotted data relevant to the construction of the Hvammsvirkjun power plant from both sides of the Thjórsá River and highlighted the tectonic structures at risk. The results of our study do not allow the prediction of future earthquakes and faulting, but they can be used to issue the following recommendations:

1. **Hazard related to the northerly faults.** Five northerly faults cross the Thjórsá River in our study area four of which stretch under, or are very near, the planned site of the Hvammsvirkjun power plant (Faults 1 to 4 on Fig. 16). These faults have dip-slip, with possible cumu-

lative vertical displacement indicating their activity through time. Furthermore, these faults present evidence of dextral strike-slip during the Holocene. The first mainshock of the 1896 earthquake sequence most likely originated on Fault 2 (the main N-S fault in Skarðsfjall), and present-day microearthquake activity indicates this fault is still active. It is recommended to avoid any construction of structures across these four faults.

2. **Hazard related to the Thjórsá River.** Our data indicate a more intense fracture network in the planned Hvammsvirkjun area south of Thjórsá River than north of the river. This is consistent with a general decrease in the intensity of tectonic activity as one moves away from the centre of the seismically active zone as also evidenced by the present microearthquake activity. ENE striking active faults are common in South Iceland and interpreted to be conjugate with the northerly fractures. Some of the ENE fractures in the Hvammsvirkjun area show evidence of recent movement and leakage. The hypothesis that the Thjórsá River follows a tectonically governed ENE-WSW lineament in this area cannot be refuted or confirmed. It is, however, recommended to avoid constructions of structures on, or adjacent to, the Thjórsá River in the portion between Fault 4 and east of Fault 1, especially south of the river (Fig. 16).

Due to the high density of Holocene surface ruptures south of the Thjórsá River and the history of fault movements there, it would, from the tectonic point of view, be preferable to locate the Hvammsvirkjun power plant in the Hreppar block north of the river. There, Holocene fault movements are less frequent or not present from the longitude of Minni-Núpur eastward. From this point of view, the best site for the power plant would be between Faults 4 and 5 north of the river (Fig. 16).

If the power plant cannot be located north of Thjórsá River but has to be constructed south of it, four considerations are recommended:

- a. Building structures should be placed between northerly faults, preferably between those faults that do not present leakage or evidence of recent movements.
- b. Building structures should be designed to withstand major earthquakes as well as leakages on fractures.
- c. Major Holocene surface ruptures are less present in the “NE block” of Skarðsfjall. In view of the construction costs and the risk of structures built in the faulted area between faults 1 and 4, we propose that one considers the feasibility of building structures of the water intake and the power plant in the NE block east of fault 4, discharging the outlet water through a tunnel across the faulted region. An additional advantage of this design would be a reduction in the size of Hvammslón and its environmental impact.
- d. A network for monitoring fault movements and strain accumulation in the Hvammsvirkjun area should be established. A survey of geothermal gradients in the region might also be helpful in interpreting leakage of warm and cold groundwater.

Acknowledgments. We thank Landsvirkjun for financing the greatest part of this study, and Orkustofnun for financing a part of it. At Landsvirkjun, we wish to thank especially Guðlaugur Þórarinnsson. Many inhabitants in the field made our tasks easier by permitting us to work on their land, or by helping us when needed. Thanks are to Sigurbjörg Elmirsdóttir and Sveinn Sigurjónsson (Galtalækur), Kolbrún Sveinsdóttir and Pálmi Eyólfsson (Hvammur), and Borghildur Kristinsdóttir (Skarð). We also thank Gunnlaugur M. Einarsson for his help with the GIS in preparing Map 1.

REFERENCES

- Aronson, J.I., and Sæmundsson, K. 1975. Relatively old basalts from structurally high areas in central Iceland. *Earth and Planetary Science Letters*, 28, p. 83–97.
- Einarsson, P. 1991. Earthquakes and present-day tectonism in Iceland, *Tectonophysics*, 189, p. 261–279.
- Einarsson, P., Böttger, M., and Þorbjarnarson, S. 2002. Faults and fractures of the South Iceland Seismic Zone near Þjórsá. Science Institute University of Iceland, Report in LV-2002/090, 8 p.
- Friðleifsson, I.B., Haraldsson, G.I., Georgsson, L.S., Gunnlaugsson, E., and Björnsson, B.J. 1980. Jarðhiti í Gnúpverjahreppi, Heildarkönnun. Orkustofnun, report OS80010/JHD06, 136 p.
- Hjartarson, Á. 1988. Þjórsárhraunið mikla, stærsta nútímahraun jarðar. *Náttúrufræðingurinn*, 58 (1), p. 1–16.
- Hjartarson, Á., and Snorrason, S. P. 2001. Búðafoss-Núpur. Skýringar með jarðfræðikorti. Orkustofnun report, OS-2001/070, 21 p.
- Jóhannesson, H., Jakobsson, S. P., and Sæmundsson, K. 1982. Geological map of South Iceland, sheet 6. 1:250.000. Published by Icelandic Museum of Natural History, Iceland Geodetic Institute.
- Khodayar, M., and Einarsson, P. 2002. Structural analysis of the Núpur area, Gnúpverjahreppur, South Iceland. Report for the National Power Company of Iceland (Landsvirkjun), RH-08-2002, Raunvísindastofnun Háskólans, Science Institute, University of Iceland. This report is published by Landsvirkjun under the following number, LV-2002/101 (16 p., 13 Figs., 4 photo plates, 2 maps).
- Khodayar, M., and Franzson, H. 2004. Stratigraphy and tectonic of eastern Núpur/Western Hagafjall in Gnúpverjahreppur, South Iceland. Report *Íslenskrar orkurannsóknir*, ÍSOR-2004/017, 42 p., 2 maps. Prepared for the National Power Company, National Energy Authority, and Reykjavík Energy.
- Khodayar, M., and Einarsson, G.M. 2006. Tectonic lineament map of South Iceland between Sultartangi and Thingvellir, 1:125.000. Short report *Íslenskrar orkurannsóknir*, ÍSOR-06145, 4 p. Prepared for the National Power Company, Reykjavík Energy, and National Energy Authority under the cooperative project "Bergsprungur".
- Khodayar, M. and Franzson, H. 2007. Fracture pattern of Thjórárdalur central volcano with respect to rift-jump and a migrating transform zone in South Iceland. *Journal of Structural Geology*, Vol 29, p. 898-912.
- Kristjánsson, L., Duncan, R.A., and Guðmundsson, A. 1998. Stratigraphy, paleomagnetism and age of volcanic in the upper regions of Þjórsárdalur valley, central southern Iceland. *Boreas*, Vol. 27, p. 1-13.
- Kristinsson, S.G. 2004. Jarðfræðikortlagning á Skarðsfjalli í Landssveit. BS ritgerð, Háskóli Íslands, Reykjavík, 29 p.
- Sæmundsson, K. 1970. Interglacial Lava Flows in the Lowlands of Southern Iceland and the Problem of Two-Tiered Columnar Jointing. *Jökull*, 20, p. 62–77.
- Thoroddsen, Th. 1899. Landskjálftar á Suðurlandi. Hið íslenska bókmenntafélag, Kaupmannahöfn, 269 p.

Figures

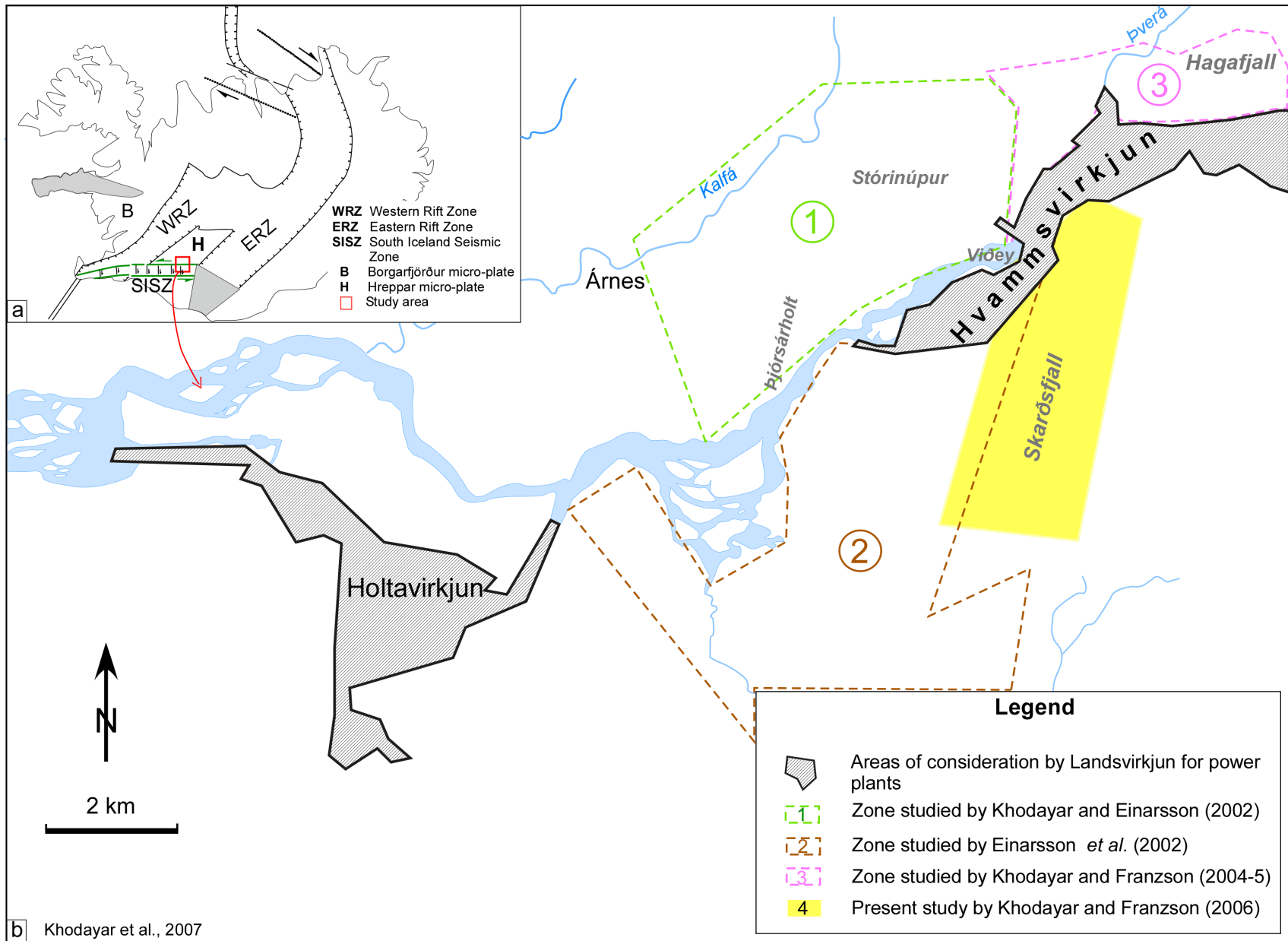


Fig. 1. Location of the study area with respect to hydropower plant projects on Thjórsá River.

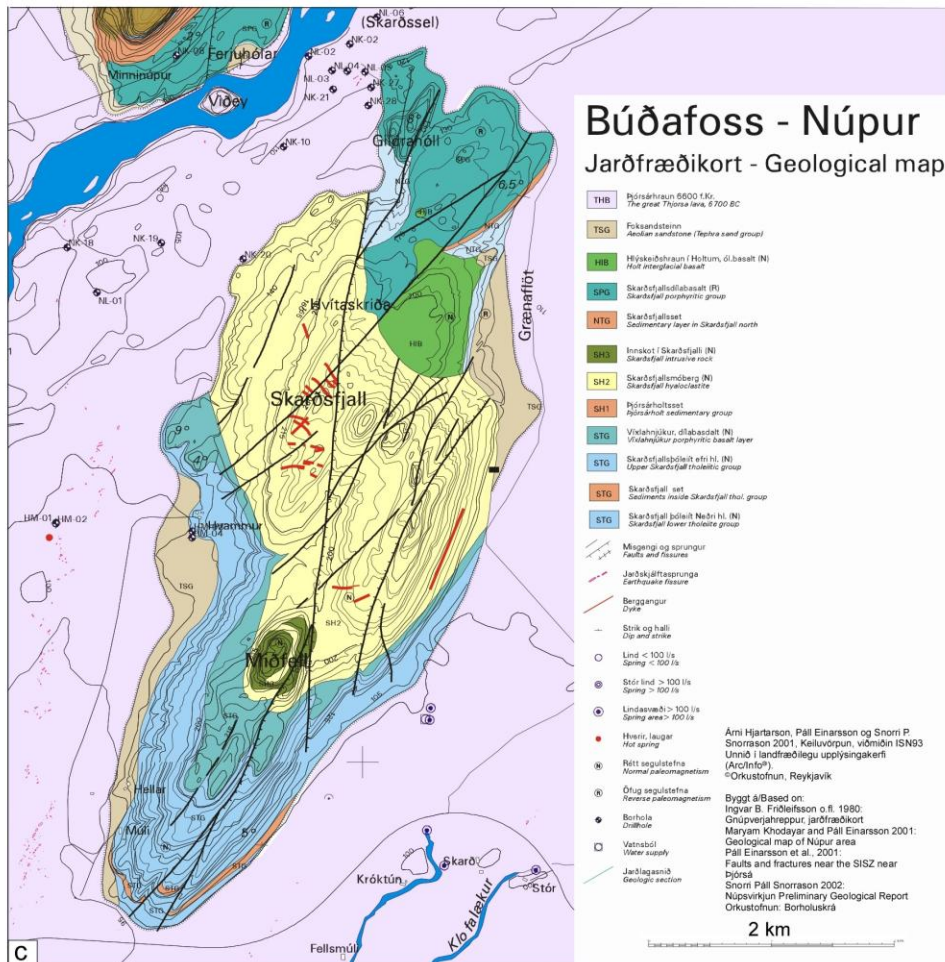
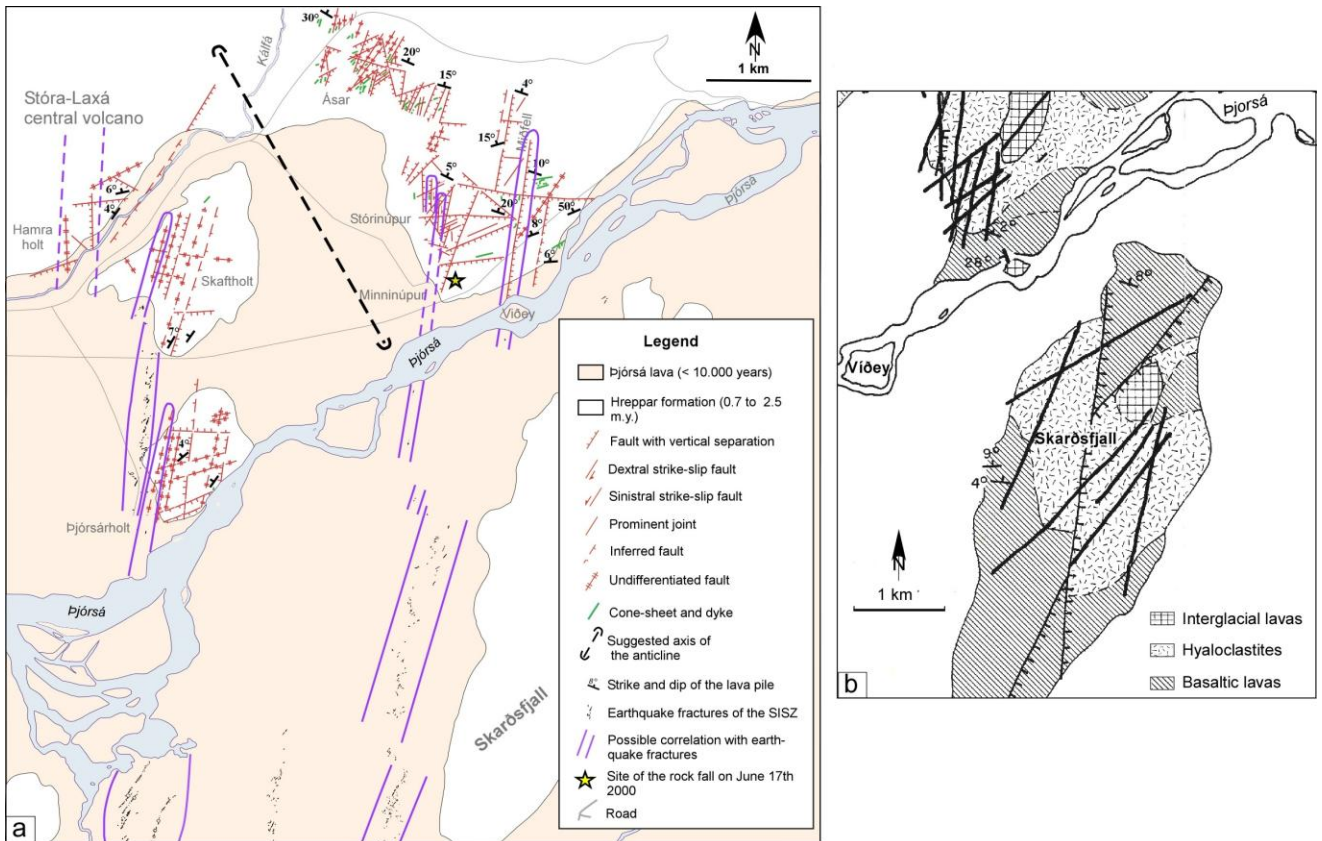


Fig. 2 (a). Structural map of the Núpur area and correlation with Holocene surface ruptures in the SISZ after Khodayar and Einarsson, 2002. (b) Geological map of Skarðsfjall and surrounding after Friðleifsson et al., 1980. (c) Geological map of Skarðsfjall after Hjartarson and Snorrason, 2001.

Fig. 3

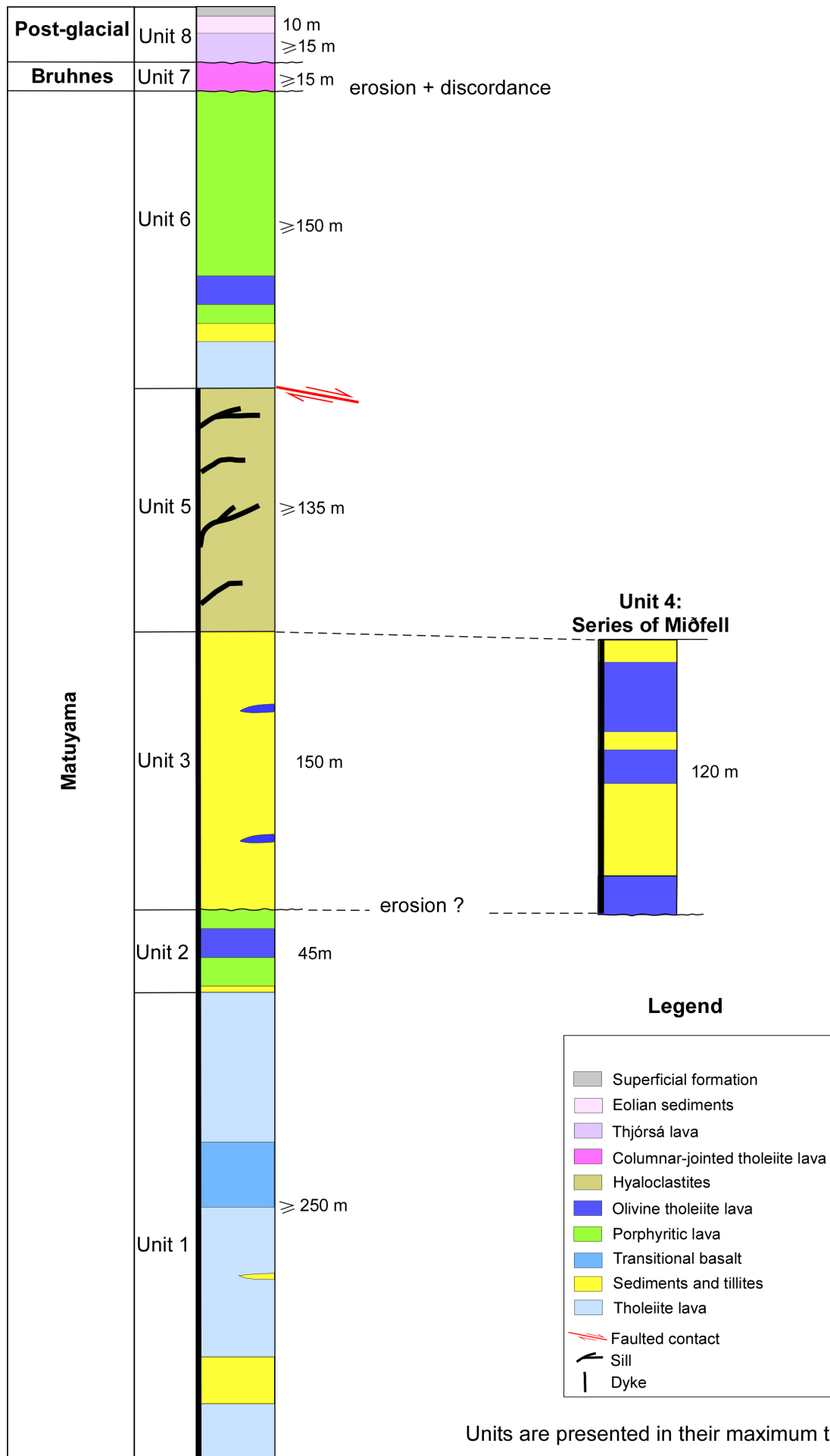


Fig. 3. Synthetic stratigraphical column of rock formations in Skarðsfjall.



Fig. 4. Stratigraphical succession. (a) View on Units 1, 2, 3 and 5 on the eastern flank of Skarðsfjall; (b) Units 3, 4 (series of Miðfell) and 5, in the middle part of the mountain.



Fig. 5. Details in Unit 3. (a) Fluvio-glacial sediments in the upper part of Unit 3; (b) Tillite of Miðfell.

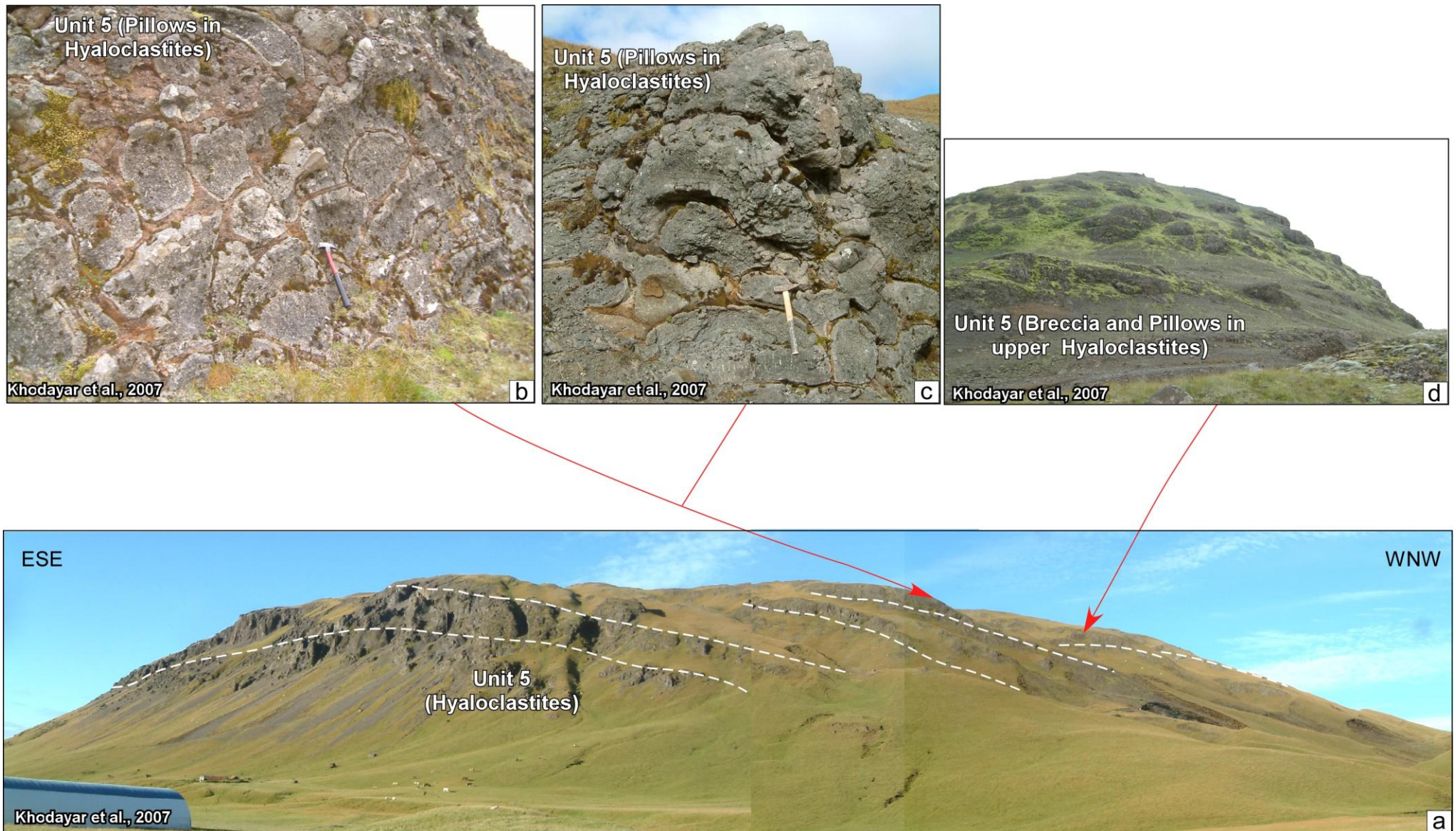


Fig. 6. Details in Unit 5: View on the hyaloclastite mountain to the north of Skarðsfjall. (a) Lenticular-shape hyaloclastite mountain showing sub-horizontal layers in the middle part and forest-bedding towards the edge of the mountain; (b and c) Pillow basalt in the middle/upper parts of Skarðsfjall; (d) Brecciated basalt in yellow tuffs in the uppermost part of the mountain.

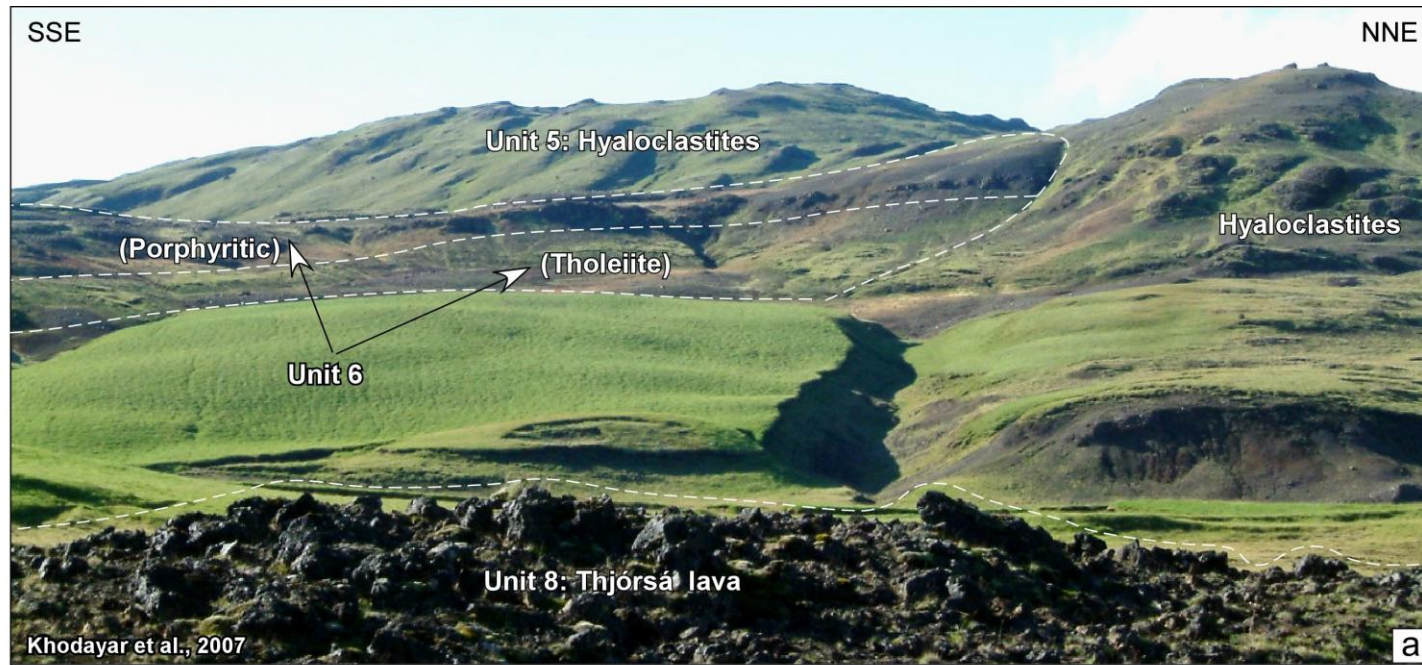


Fig. 7. Stratigraphical succession: View on the northern part of Skarðsfjall. (a) Units 5, 6, and 8; (b) Units 5, 6 and 7.

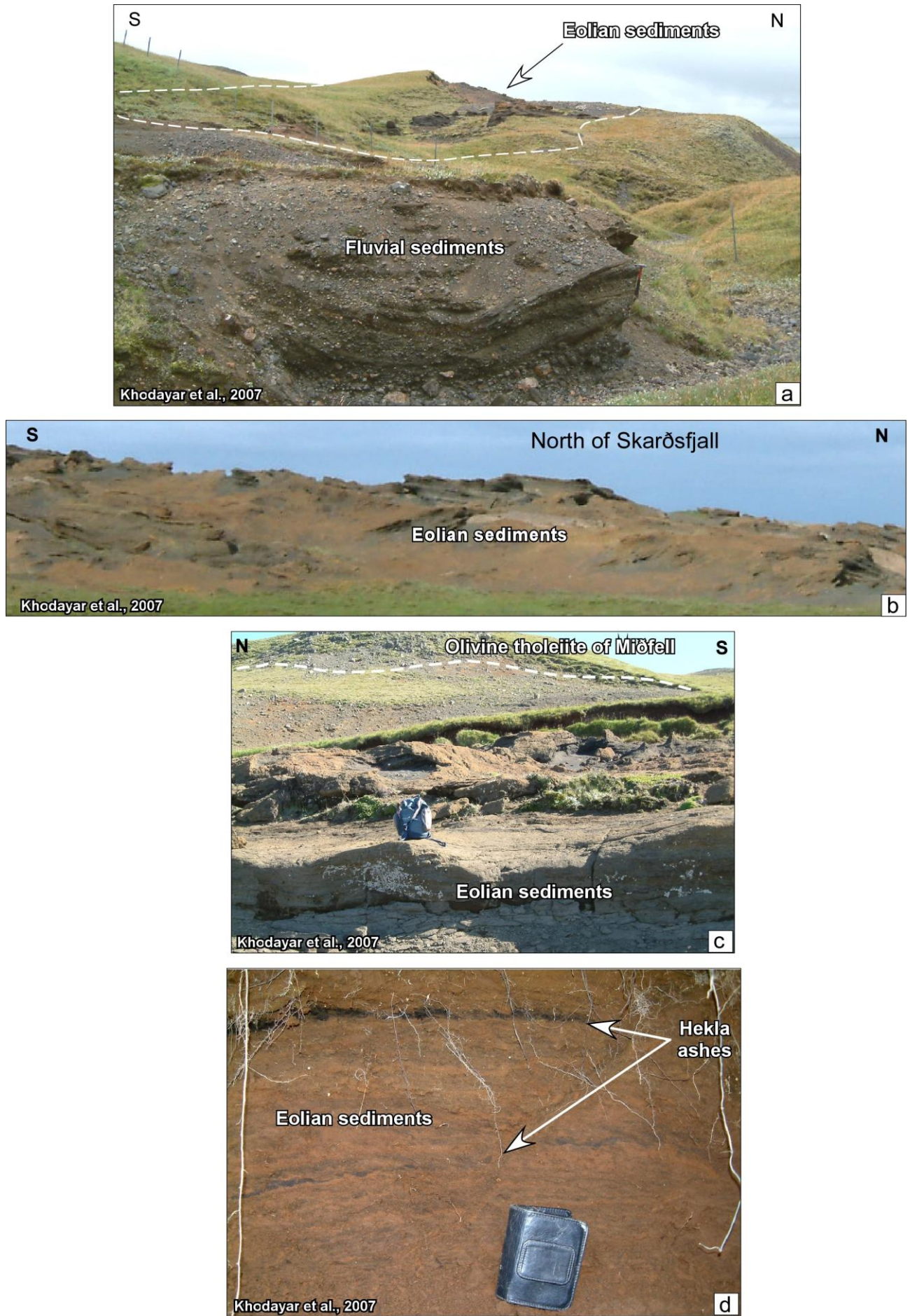


Fig. 8. Post-glacial formations: (a) Fluvial sediments under eolian sediments in the central valley in Skarðsfjall; (b) Eolian sediments; (c) Eolian sediments in the western flank of Skarðsfjall on the slope of Miðfell; (d) Close-up view on eolian sediments containing several Hekla ash layers.

-  Normal fault; bars toward the down-thrown block
-  Dextral strike-slip fault

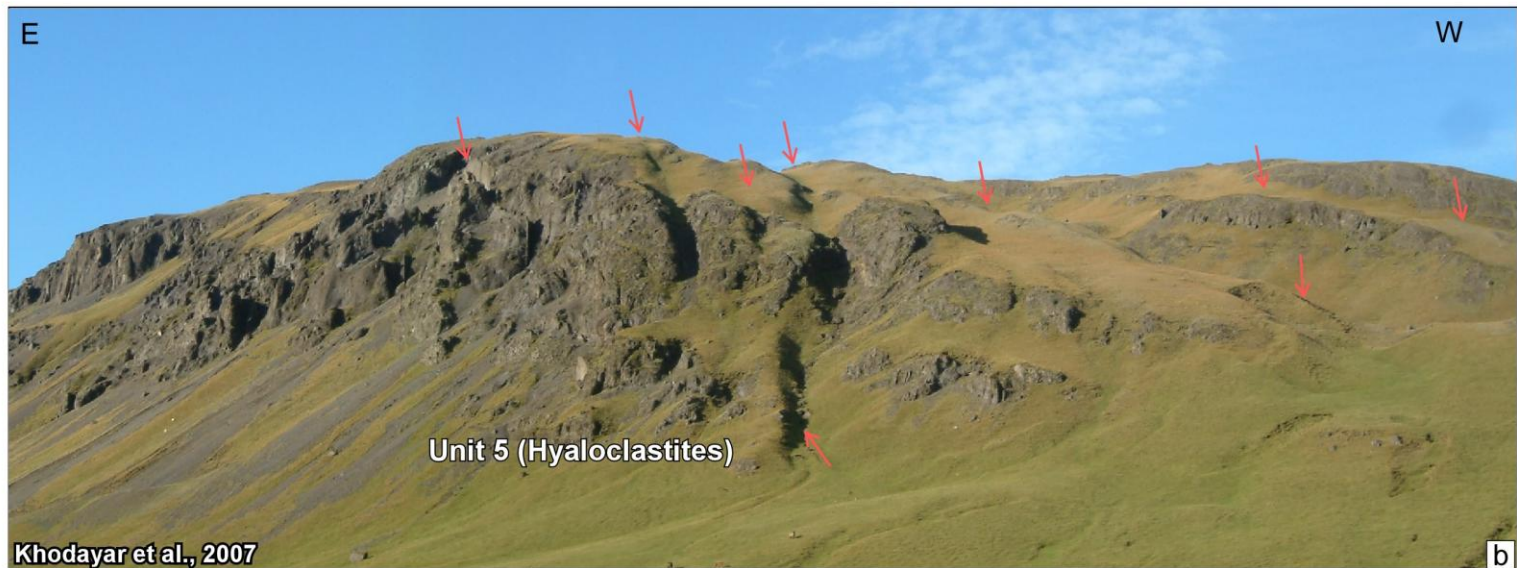
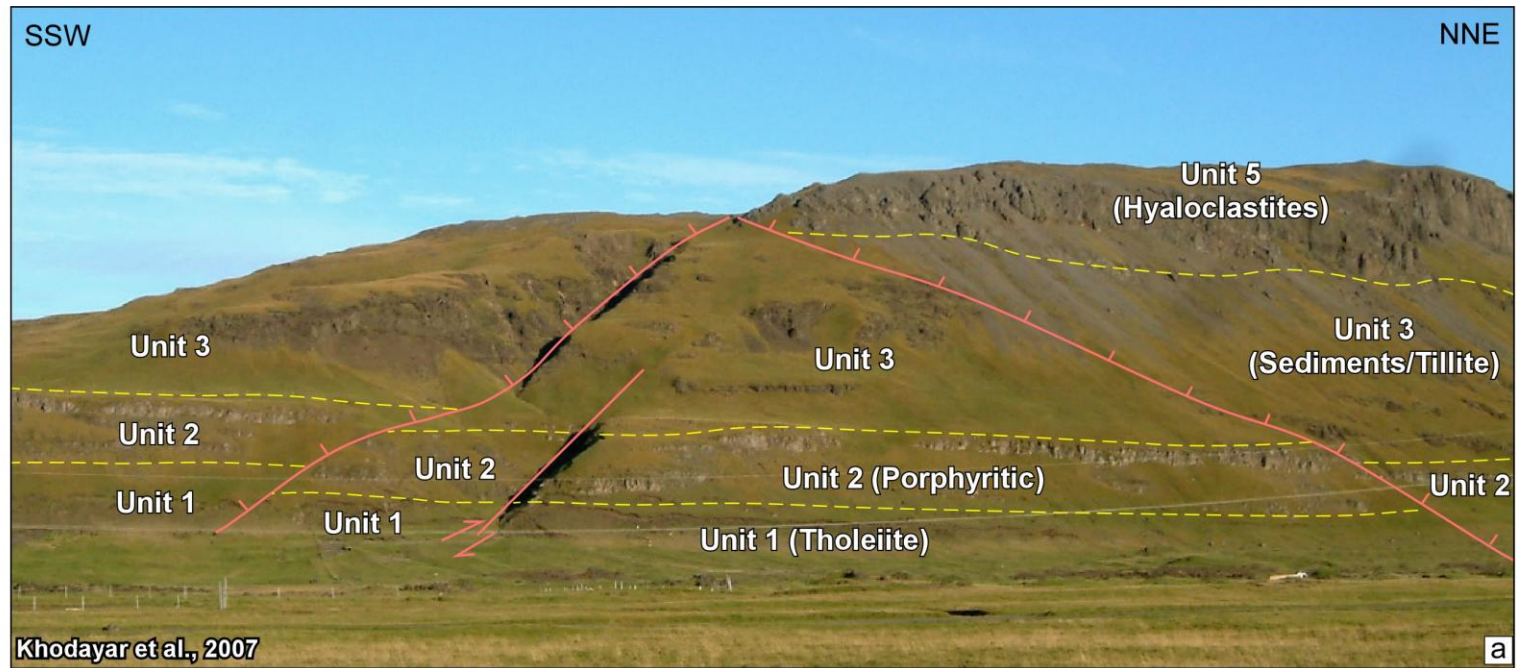


Fig. 9. Basement Faults: (a) Faults displacing various units; (b) Undifferentiated fractures in the hyaloclastites.

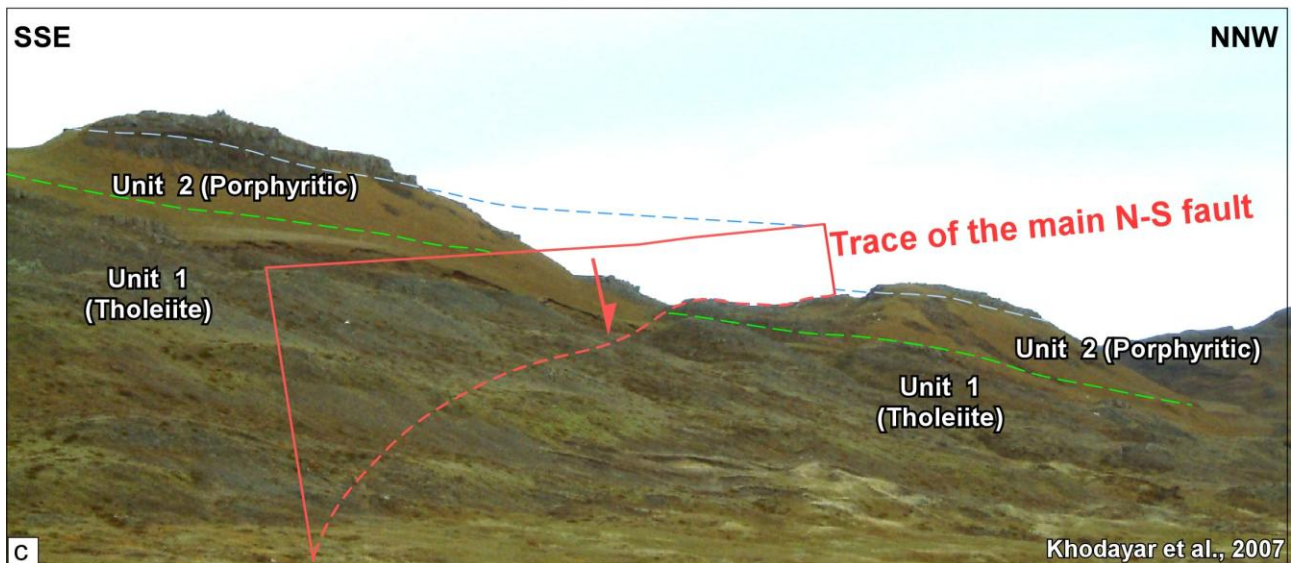
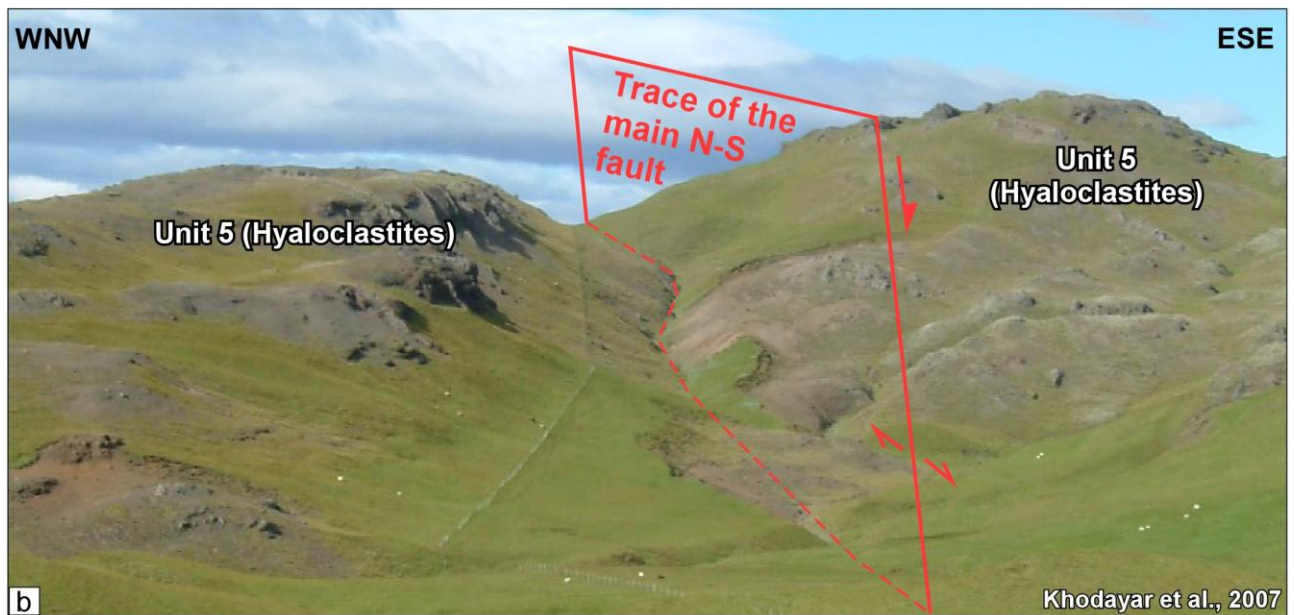
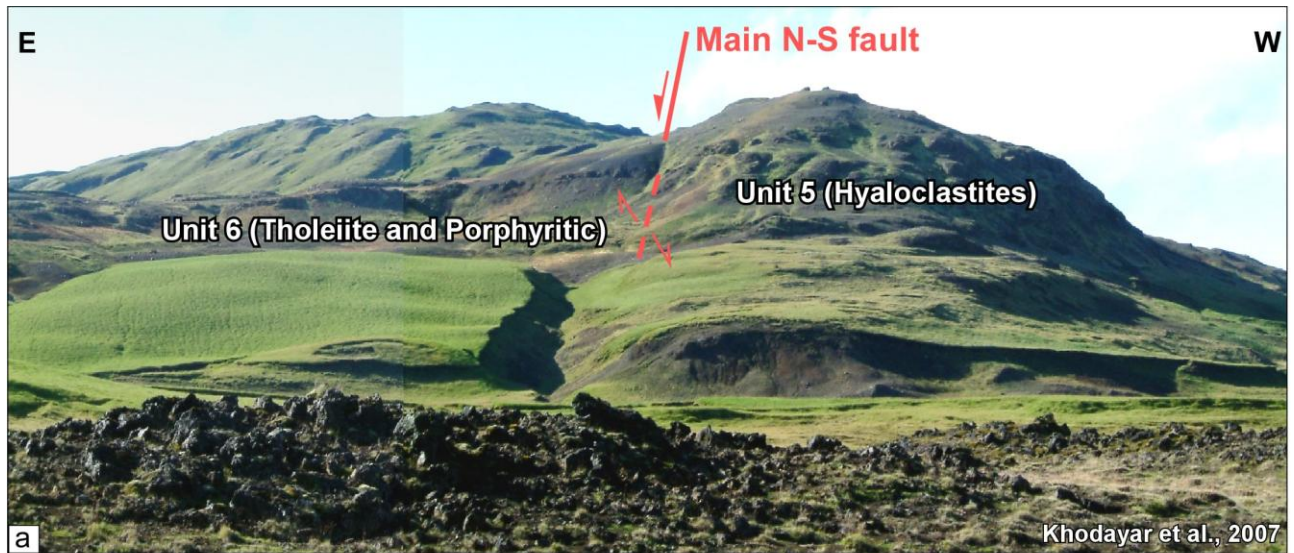


Fig. 10. Basement Faults: View on the main N-S Fault. (a) North of Skarösfjall, the fault plane as the contact between Units 5 and 6; (b) In the median valley, the trace of the fault is seen in the hyaloclastites; (c) In its southern portion, the main N-S fault displaces Units 1 and 2 by 25 m down to the east.



Fig. 11. Dykes (1). (a and b) Northerly dykes in the hyaloclastites presenting pillowy-edges; (c and d) NNW dykes in sediments/tillite of Unit 3.

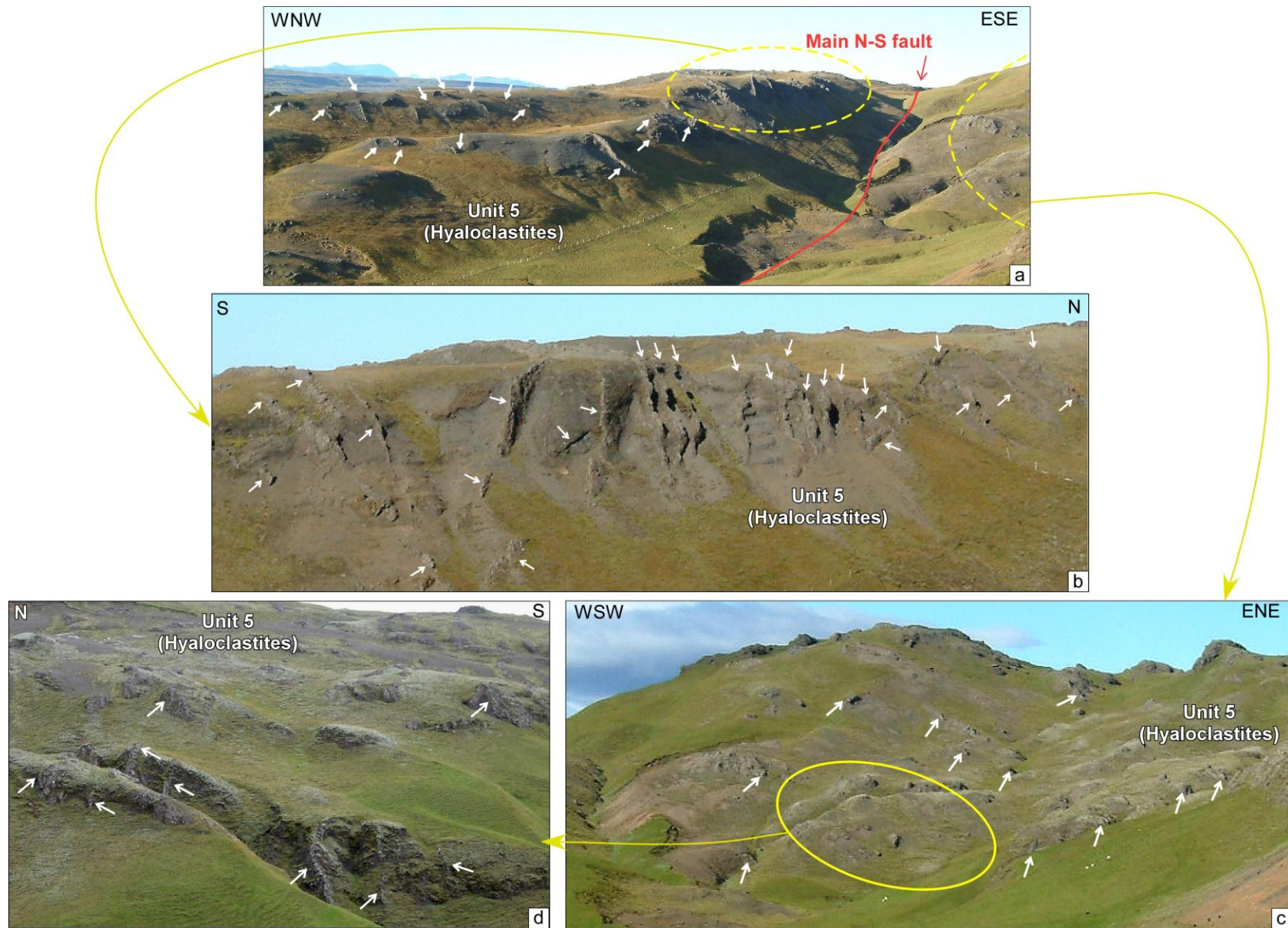


Fig. 12. Dykes (2): Feeder dykes of the hyaloclastites. (a) Mostly WNW and a few N-S dykes to the west of the main N-S fault; (b) Close-up of the dense network of WNW feeder dykes to the west of the main N-S fault; (c) Mostly NNW feeder dykes to the east of the main N-S fault; (d) A few WNW and NNW feeder dykes to the east of the main N-S fault.



Fig. 13. Holocene fault movements possibly during the 1896 earthquakes along the main N-S fault in Skarðsfjall (1): (a) View to the south-southwest on fault segments and push-ups in the median valley. Letter (P) indicates push-up; (b) Close-up view on dip-slip along the main N-S fault; (c) Close-up view on two sink-holes along the trace of the main N-S fault.

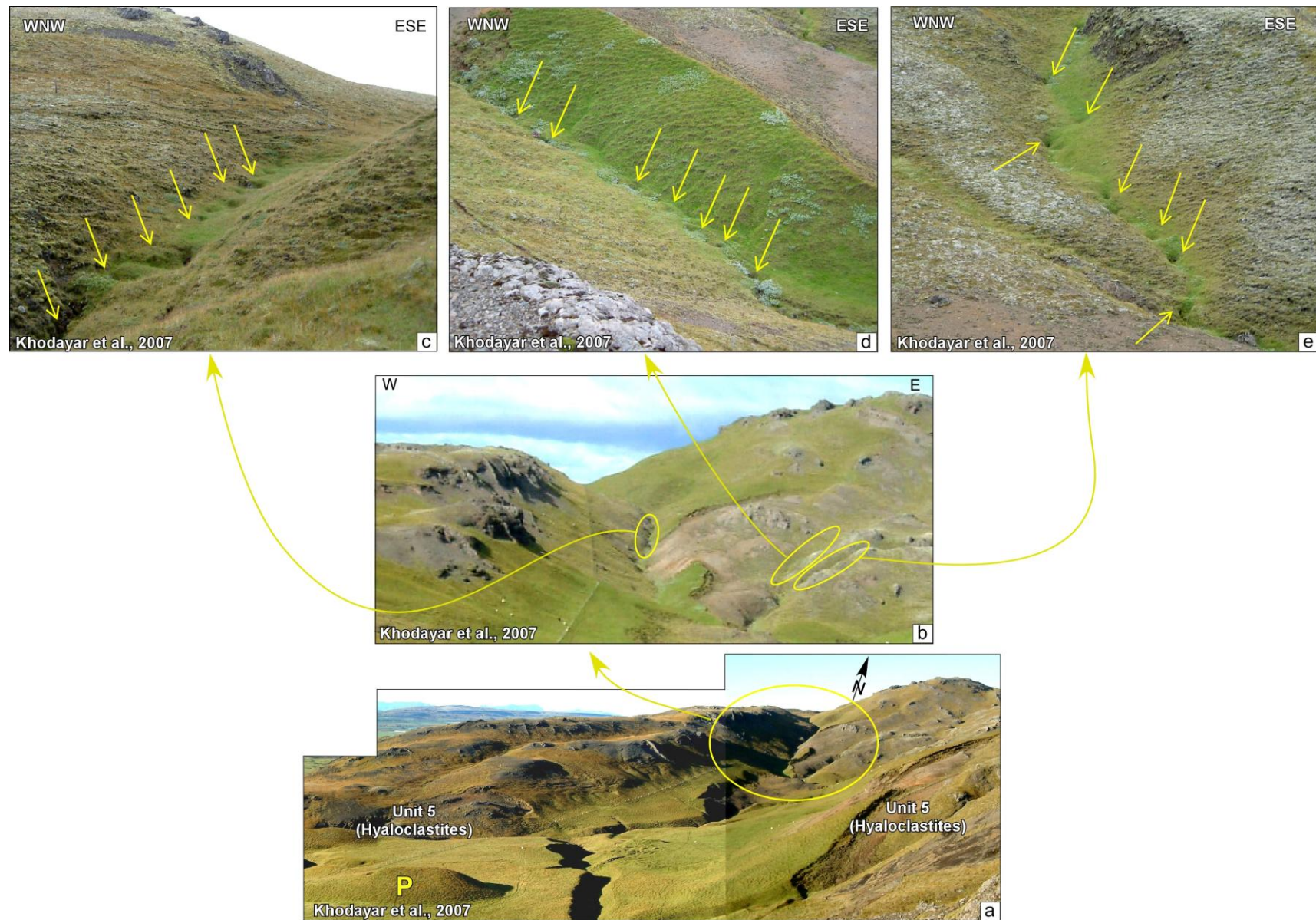


Fig. 14. Holocene fault movements possibly during the 1896 earthquakes along three northerly faults in Skarðsfjall (2): (a and b) General location of the faults in the median valley. Letter (P) indicates push-up; (c) Close-up view on sink-holes along the main N-S fault; (d and e) Close-up on sink-holes along two other northerly faults east of the main N-S fault.

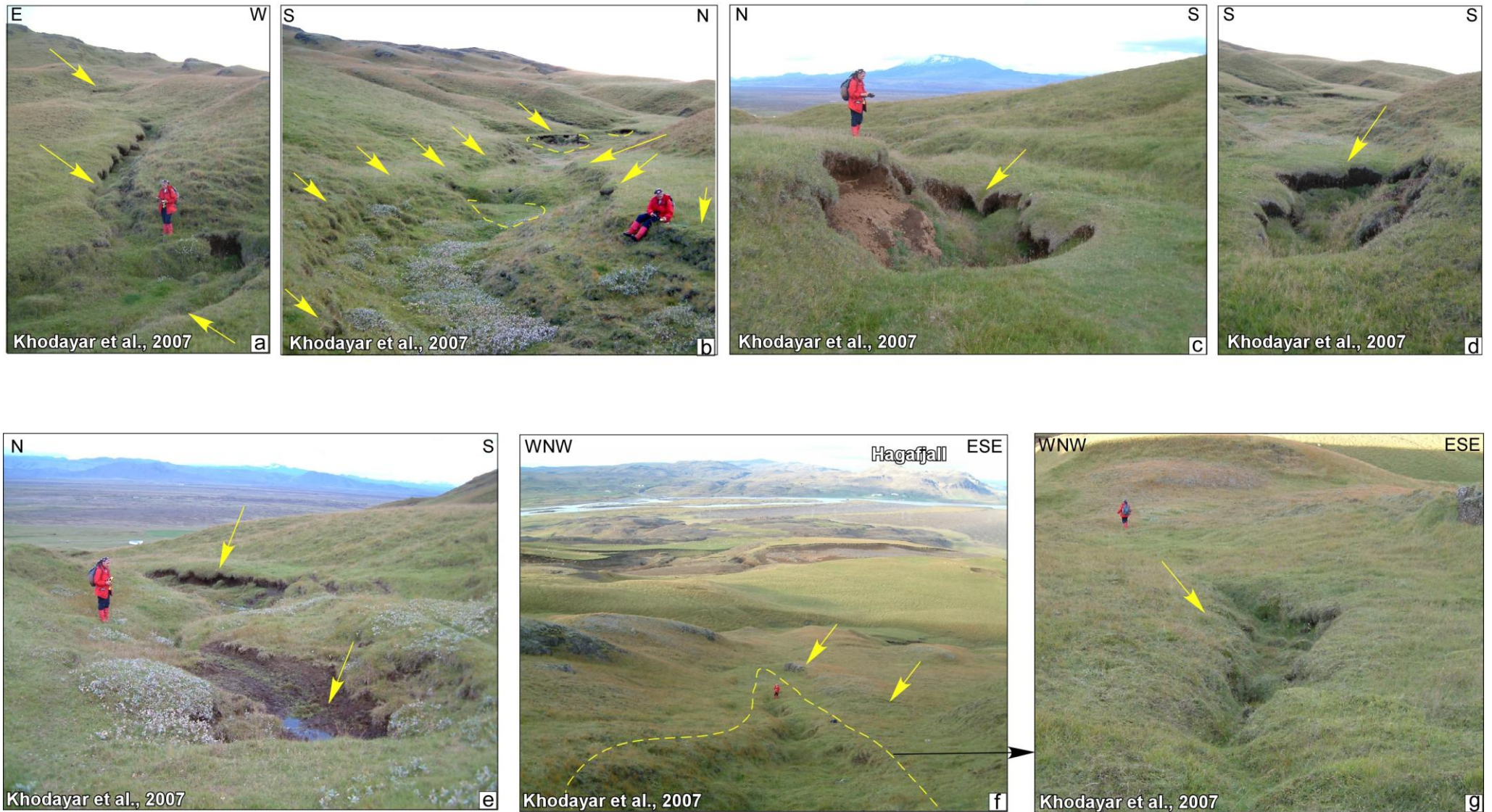


Fig. 15. Holocene fault movements possibly during the 1896 earthquakes along faults of other sets to the north of Skarðsfjall (3). (a) Fractures striking northerly and E-W; (b) Sink-holes within an E-W graben on a stepped-fault scarp; (c and d) Close-up on the size of sink-hole within the E-W striking fault; (e) Right-stepping array of sink-holes within an E-W sinistral fault; (f and g) Overview and close-up view on a NNE striking sink-hole.

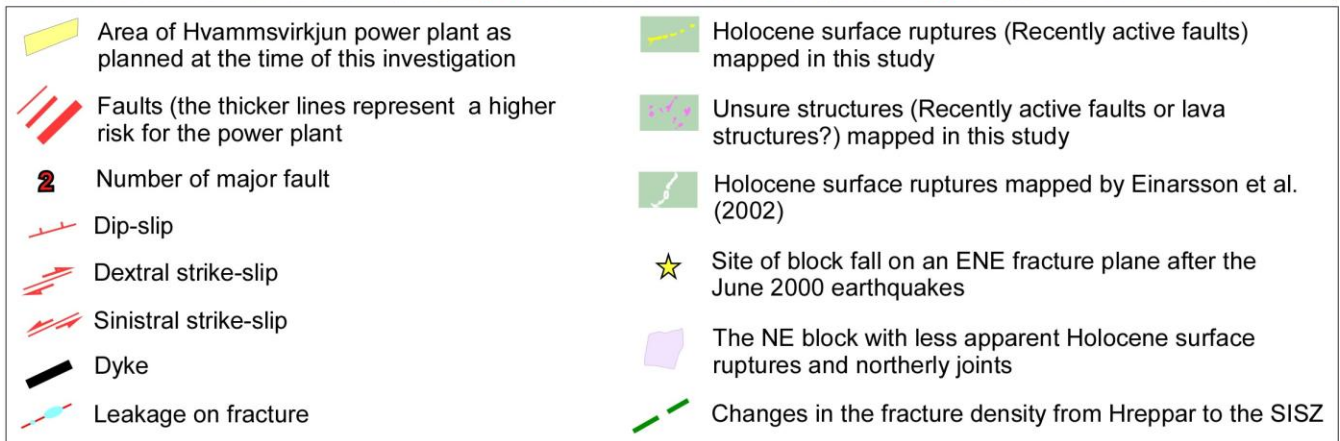
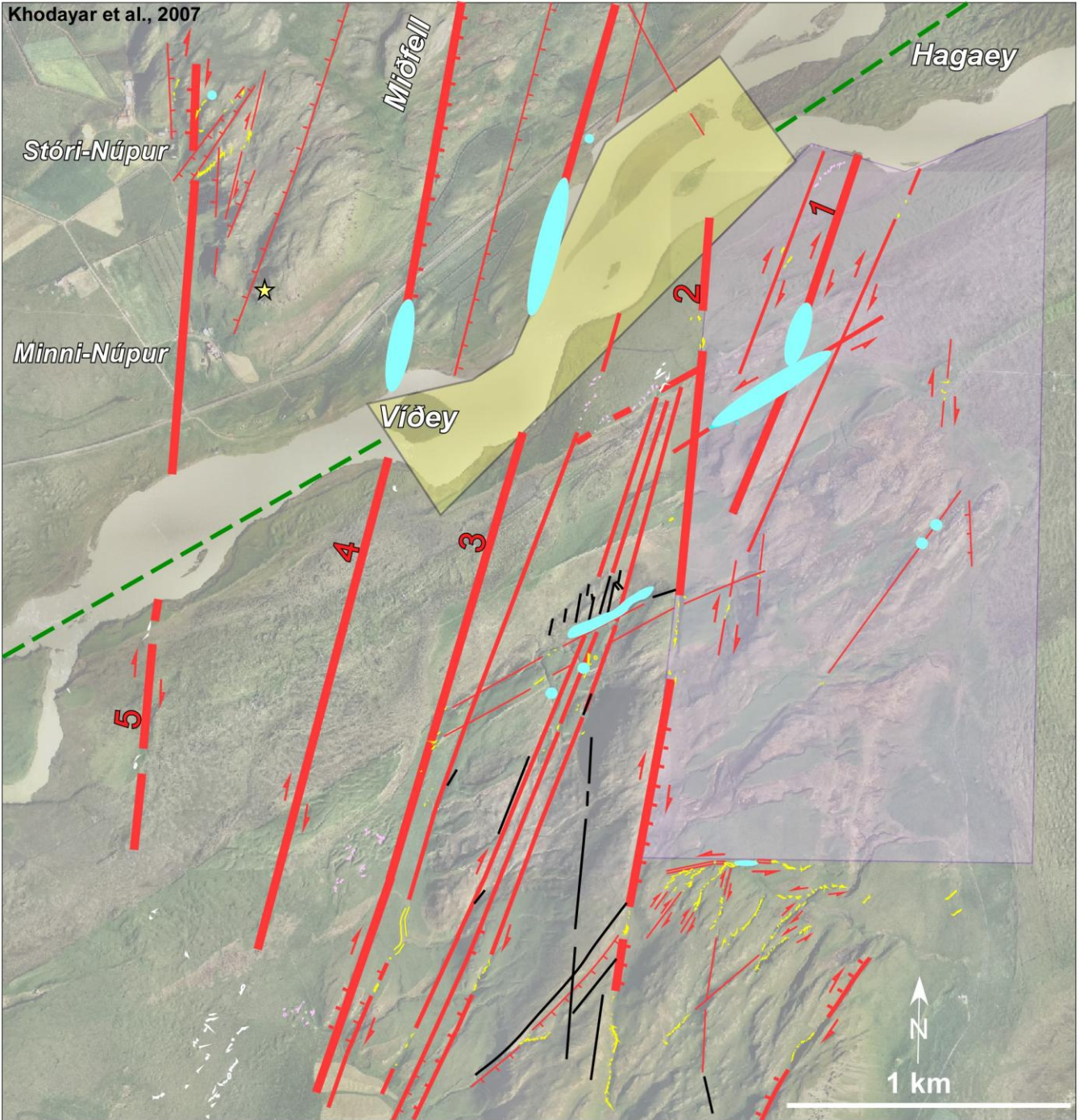


Fig. 16. Tectonic structures with potential risks at the site of the planned Hvammsvirkjun power plant.

Map 1

Geological map of Skarðsfjall

Basement tectonics, Holocene surface ruptures, Leakage, and Stratigraphy

Legend

- Holocene surface ruptures (Recently active faults) as mapped by Khodayar et al. (2006)
- Unsure structures (lava structures or Recently active faults?)
- Leakage on fractures (cold springs < 8.1°C)
- Undifferentiated fault
- Normal fault
- Dextral strike-slip fault
- Sinistral strike-slip fault
- Possible fault trace
- Dykes
- Strike and dip of the series

- Unit 8**
- SF Superficial formations
 - ES Eolian sediments and local fluvial sediments
 - ThL Thjorsá lava (8.000 yr)

- Unit 7**
- InL Interglacial columnar-jointed tholeiite lavas

- Unit 6**
- Po4 Porphyritic lavas
 - OTh5 Olivine tholeiite lavas
 - Po3 Porphyritic lavas
 - Ti/S3 Sediments of fluvio-glacial origin
 - Th4 Tholeiite lavas

- Unit 5**
- Hy Hyaloclastites

- Unit 4 (Series of Miðfell)**
- Ti/S2 Fluvio-glacial sediments
 - OTh4 Olivine tholeiite lavas
 - Ti/S2 Fluvio-glacial sediments
 - OTh3 Olivine tholeiite lavas
 - Ti/S2 Tillite and fluvio-glacial sediments
 - OTh2 Olivine tholeiite lavas

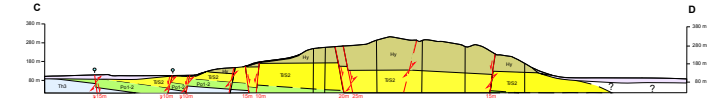
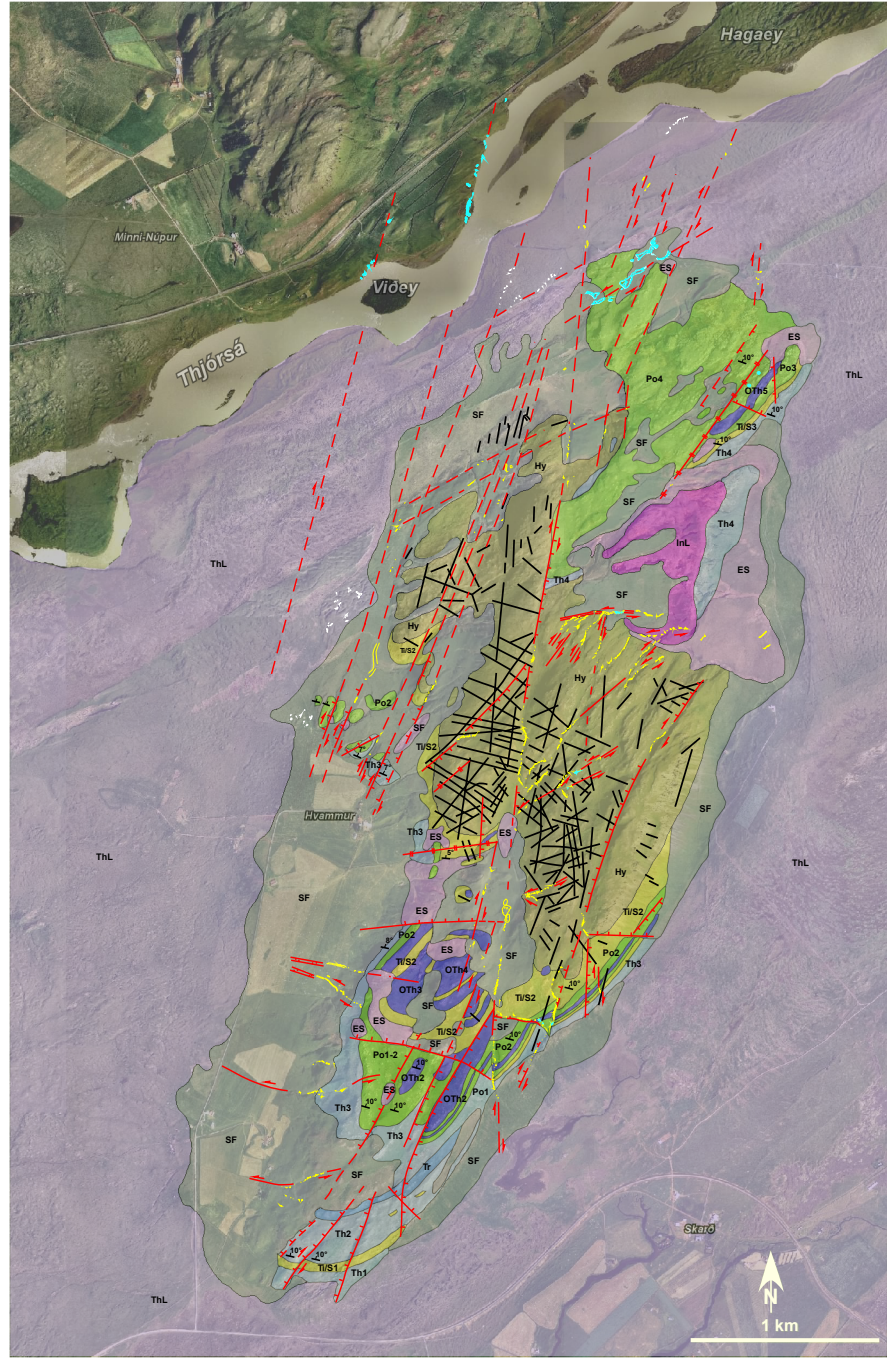
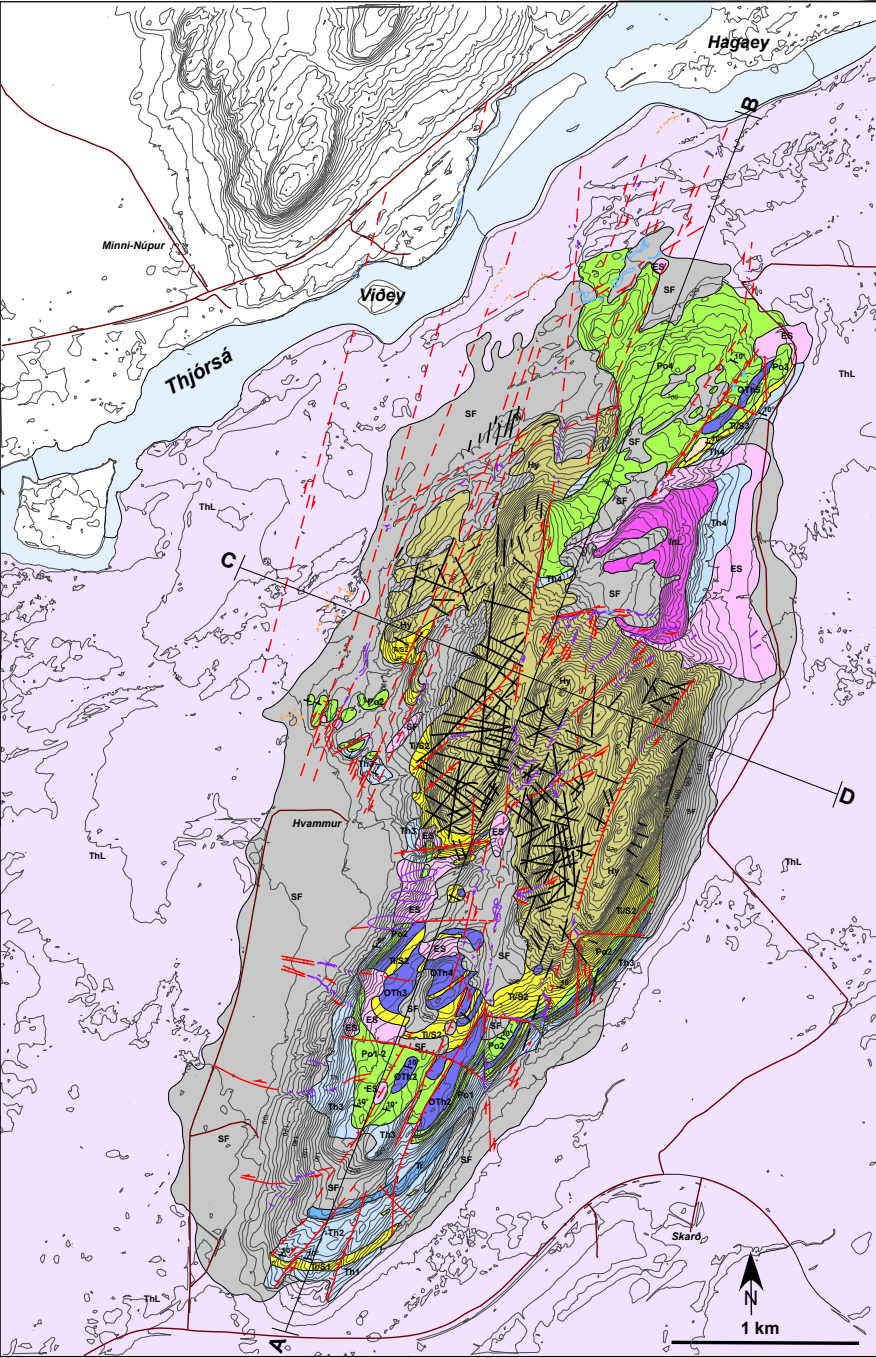
- Unit 2**
- Po2 Porphyritic lavas
 - OTh1 Olivine tholeiite lavas
 - Po1 Porphyritic lavas and local intercalation of tuffaceous sediments/hyaloclastites

- Unit 1**
- Th3 Tholeiite lavas
 - T Transitional basalt
 - Th2 Tholeiite lavas and local intercalation of tuffaceous sediments
 - Ti/S1 Tillite
 - Th1 Tholeiite lavas

Leakage on fractures shown on cross-sections

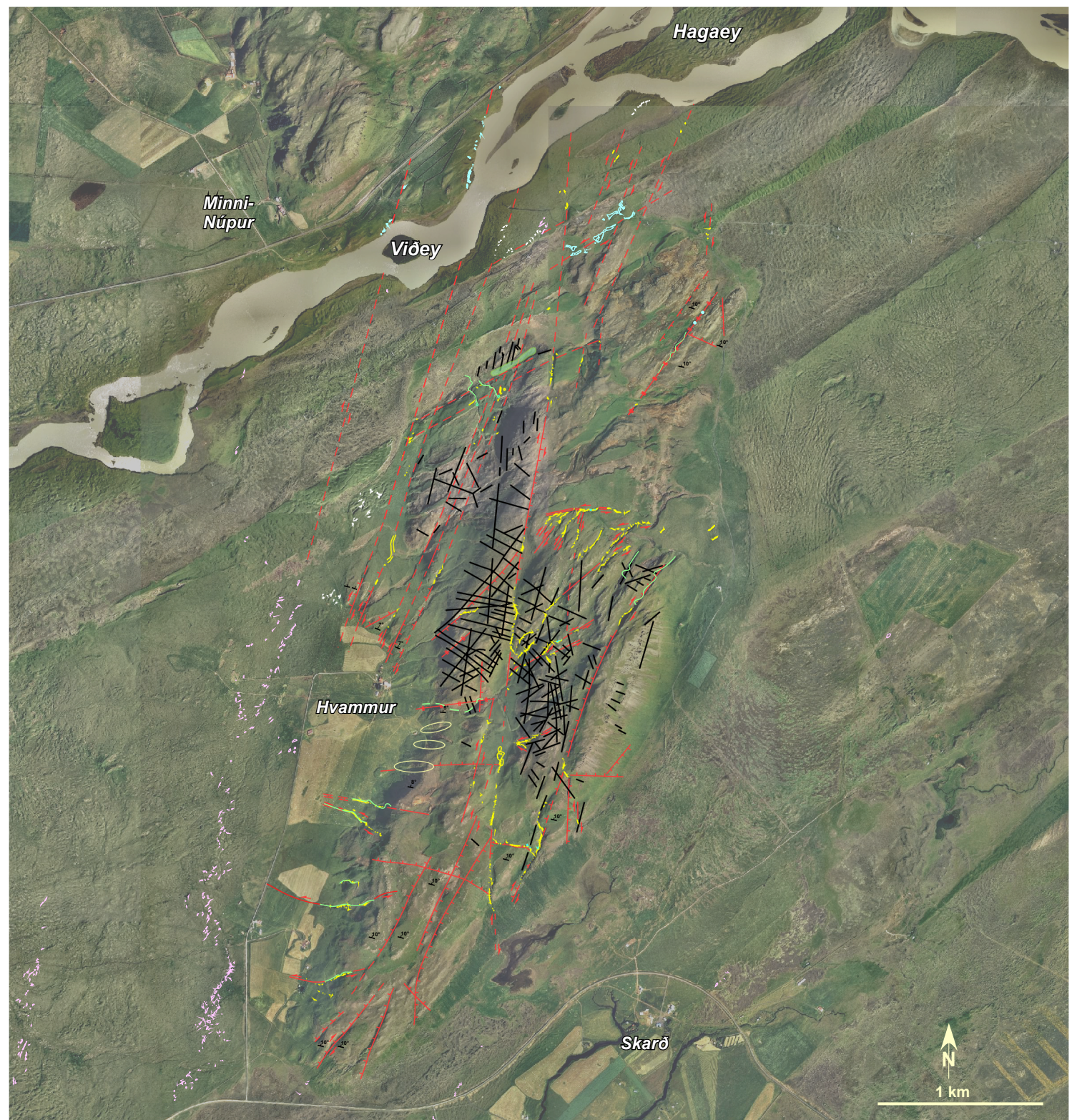
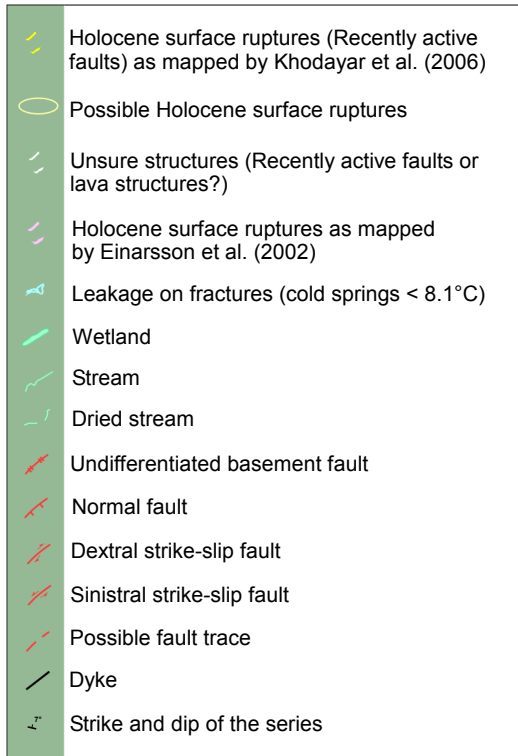
Refer to this map as:
 Maryam Khodayar, Hjalti Franzsson, Páll Einarsson, and Sveinbjörn Björnsson
 Publication: ISOR-2007/017; LV-2007/065
 Based on field mapping in 2006

Post-glacial
 Bumnes
 Matuyama



Tectonic map of Skarðsfjall

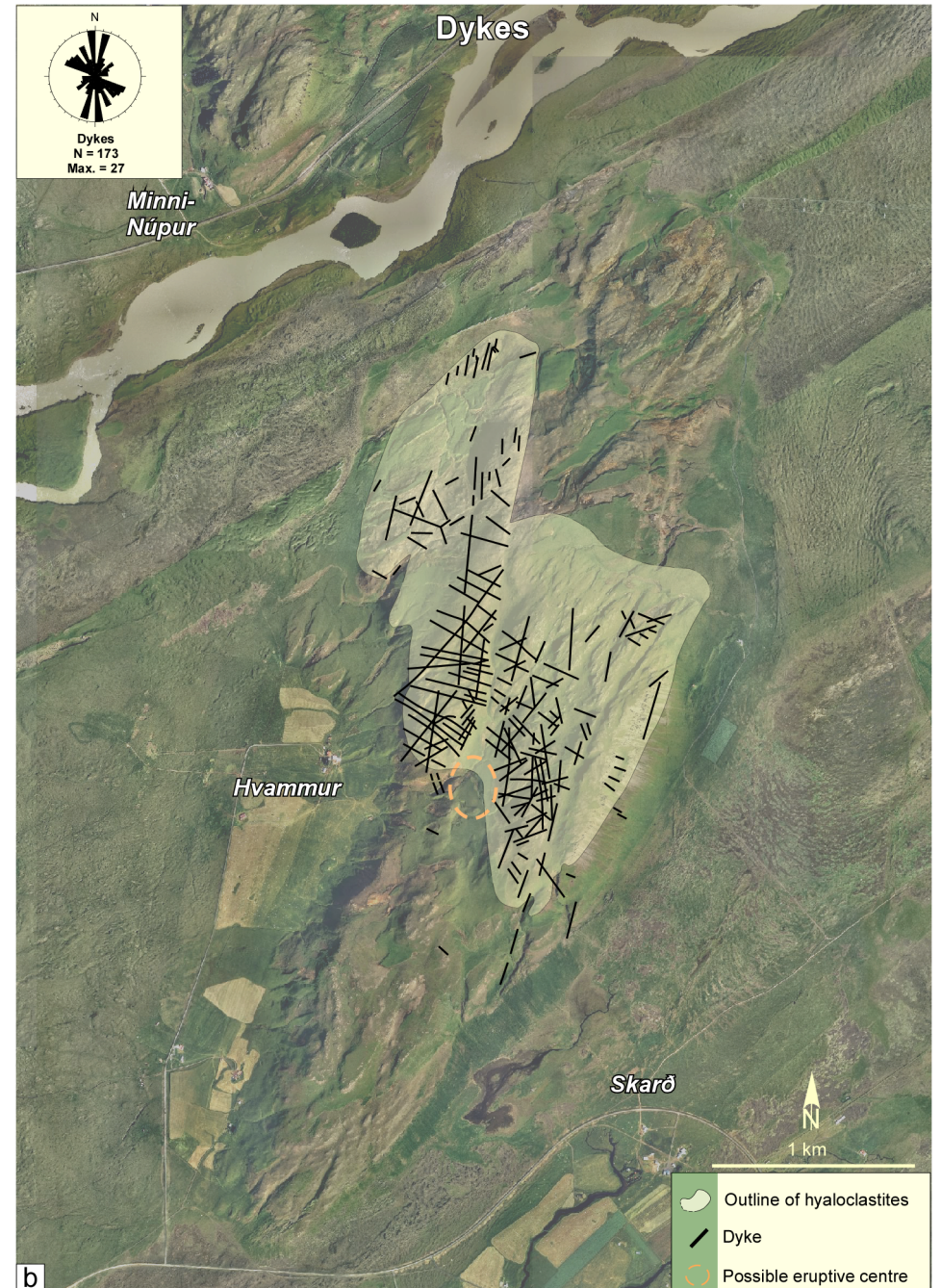
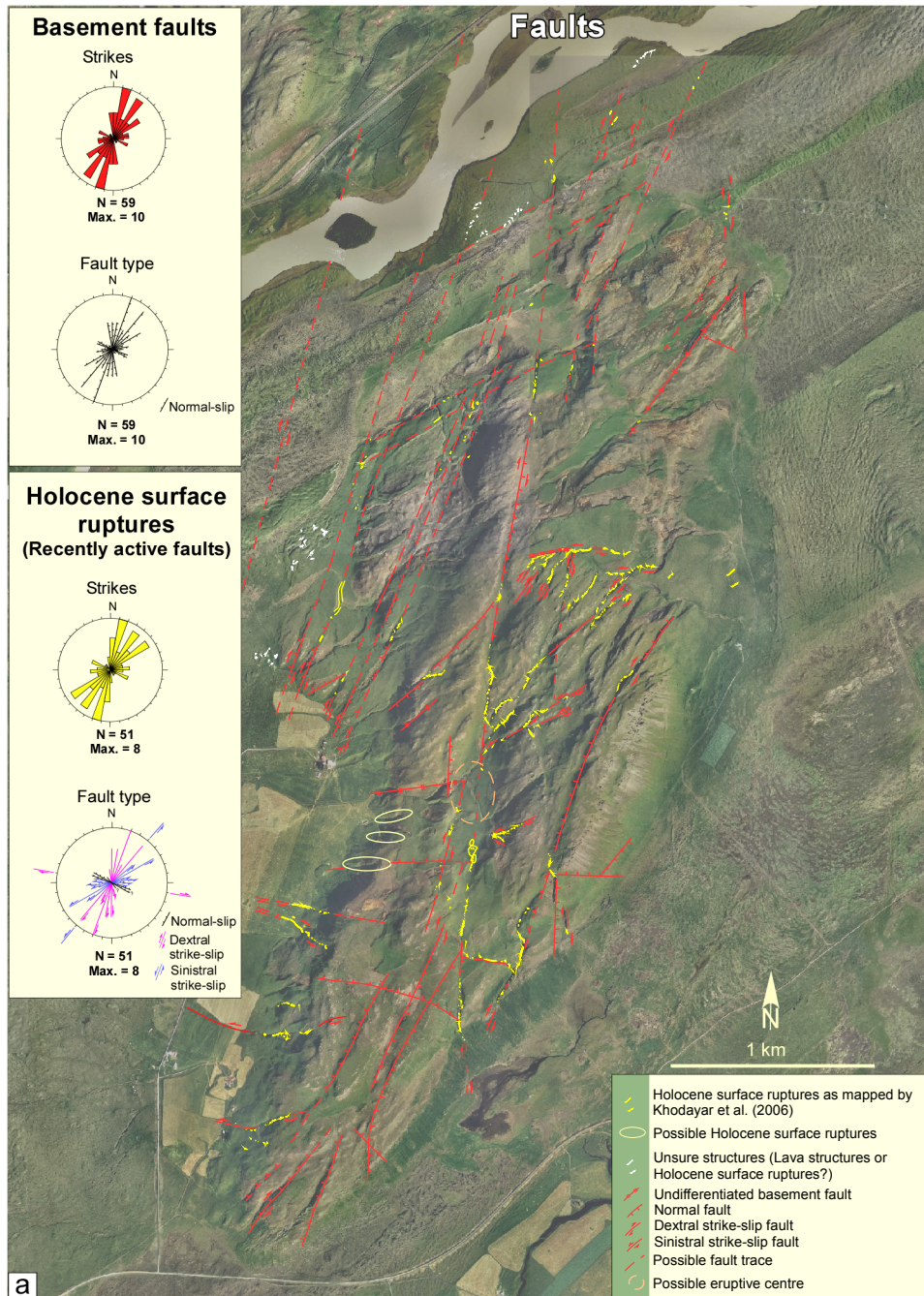
Faults, Dykes, Holocene surface ruptures, and Leakage



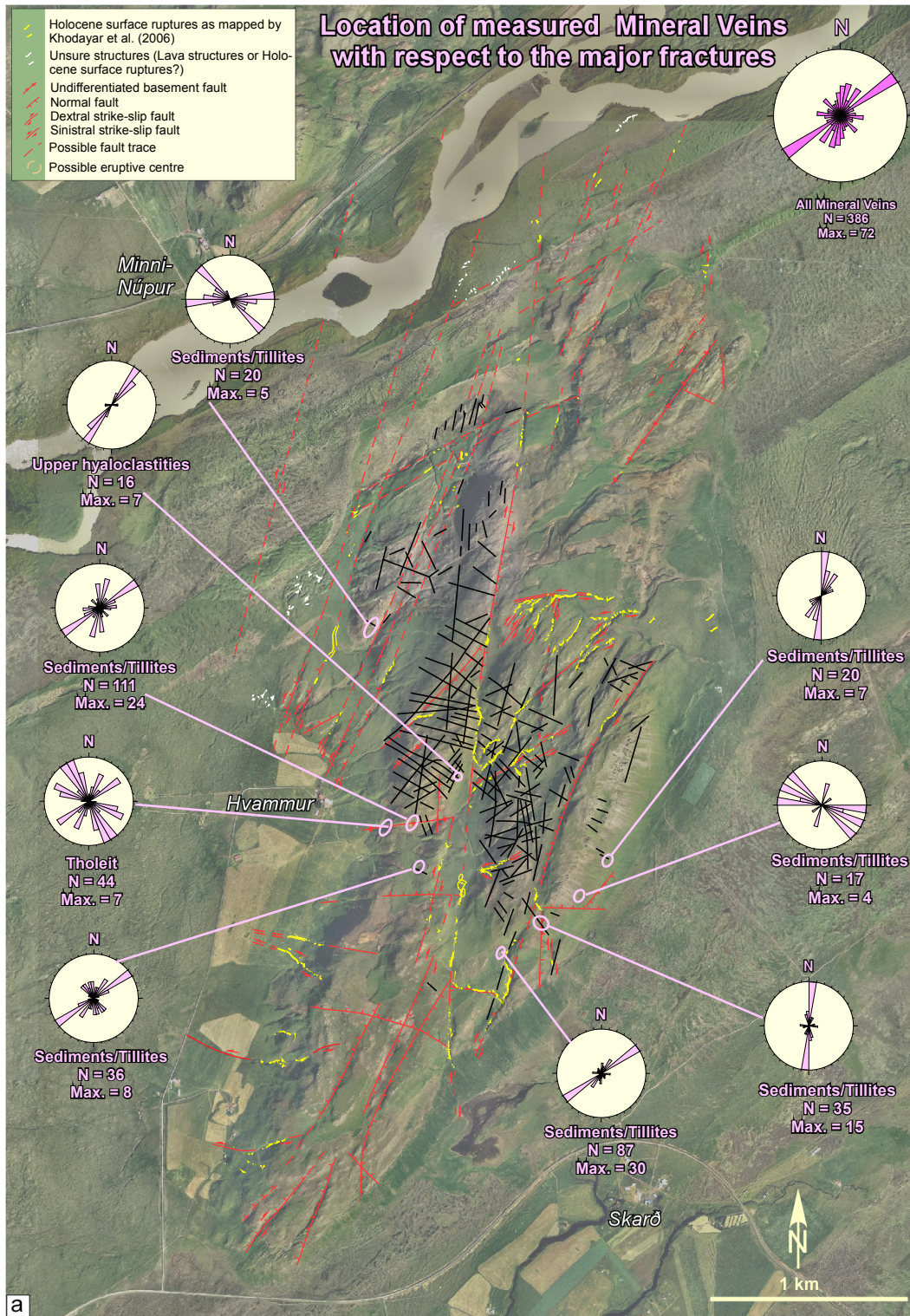
Refer to this map as:
 Maryam Khodayar, Hjalti Franzson, Páll Einarsson, and
 Sveinbjörn Björnsson
 Publication: ÍSOR-2007/017; LV-2007/065
 Based on field mapping in 2006

Faults and Dykes in Skarðsfjall

Refer to this map as:
 Maryam Khodayar, Hjalti Franzson, Páll Einarsson, and
 Sveinbjörn Björnsson
 Publication: ÍSOR-2007/017; LV-2007/065
 Based on field mapping in 2006

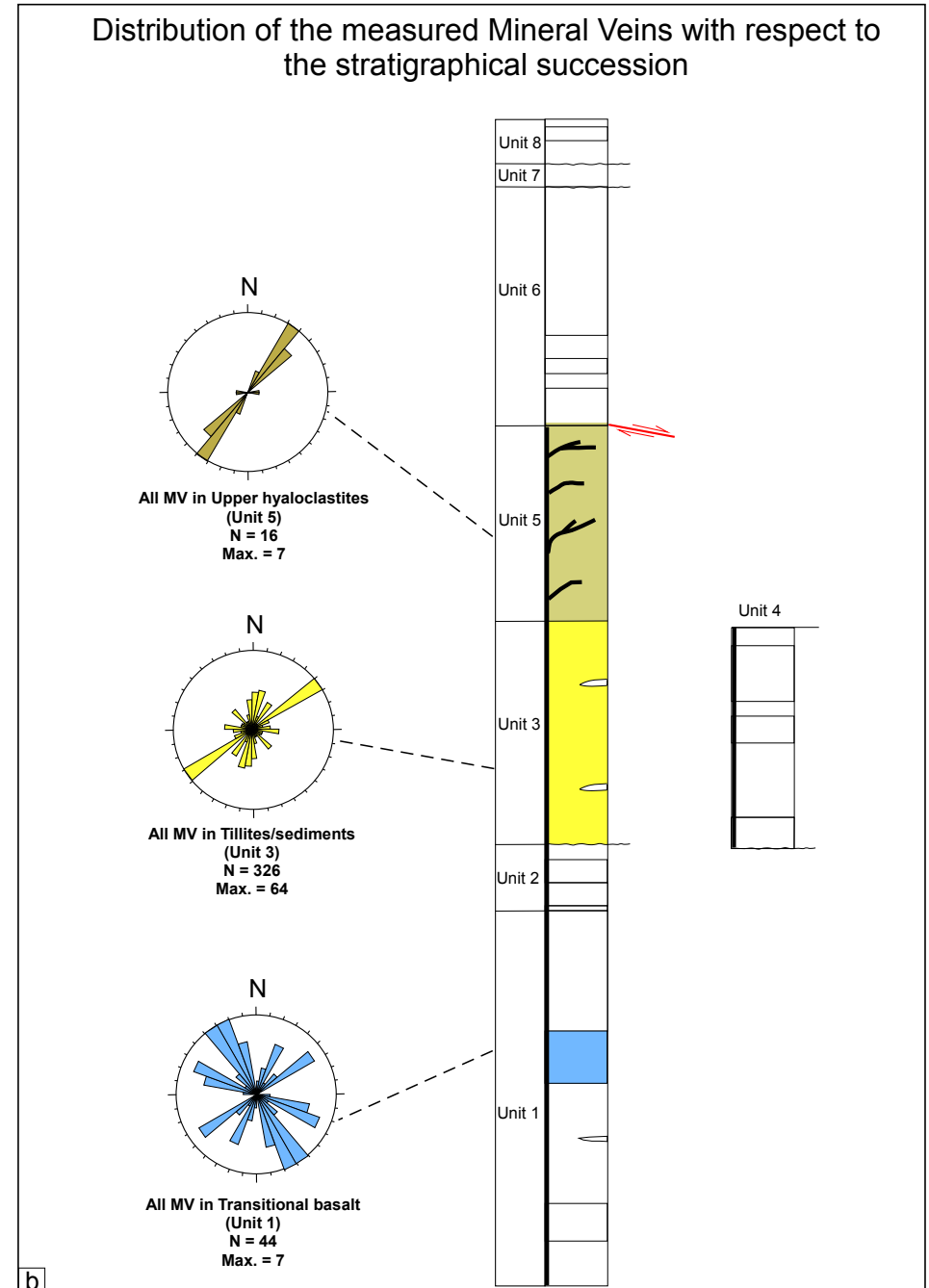


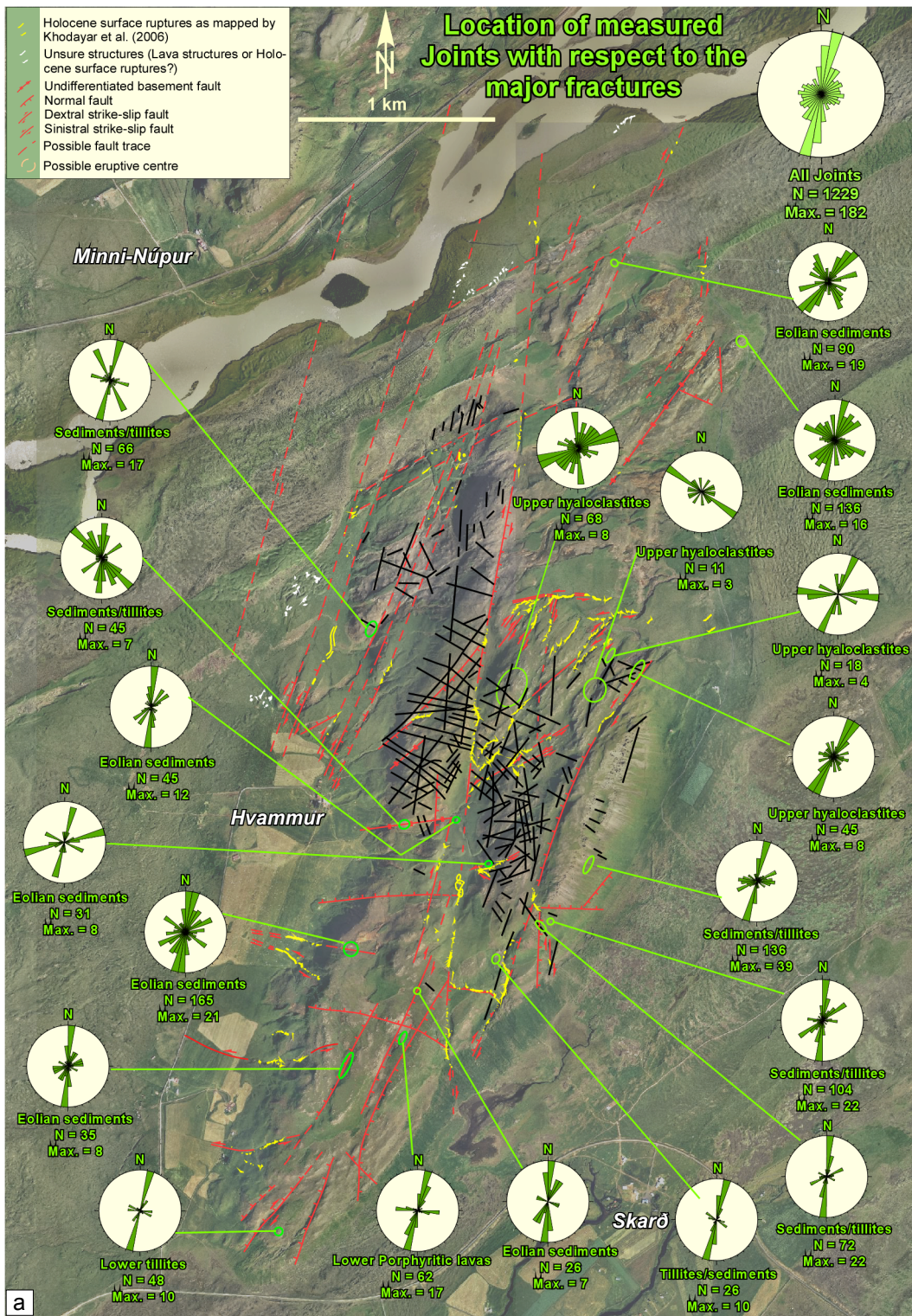
Map 4



Mineral veins in Skarðsfjall

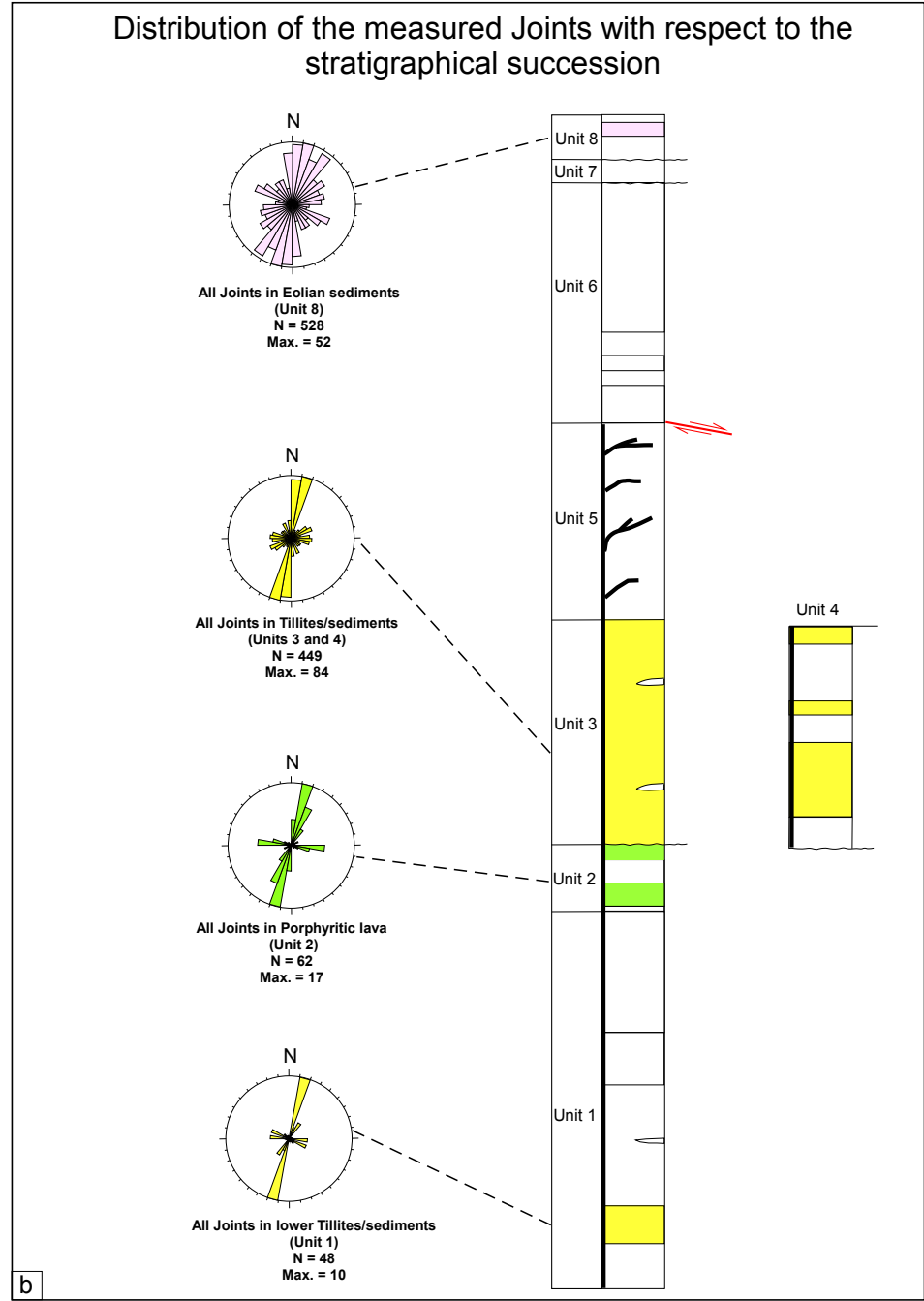
Refer to this map as:
 Maryam Khodayar, Hjalti Franzson, Páll Einarsson, and Sveinbjörn Björnsson
 Publication: ISOR-2007/017; LV-2007/065
 Based on field mapping in 2006



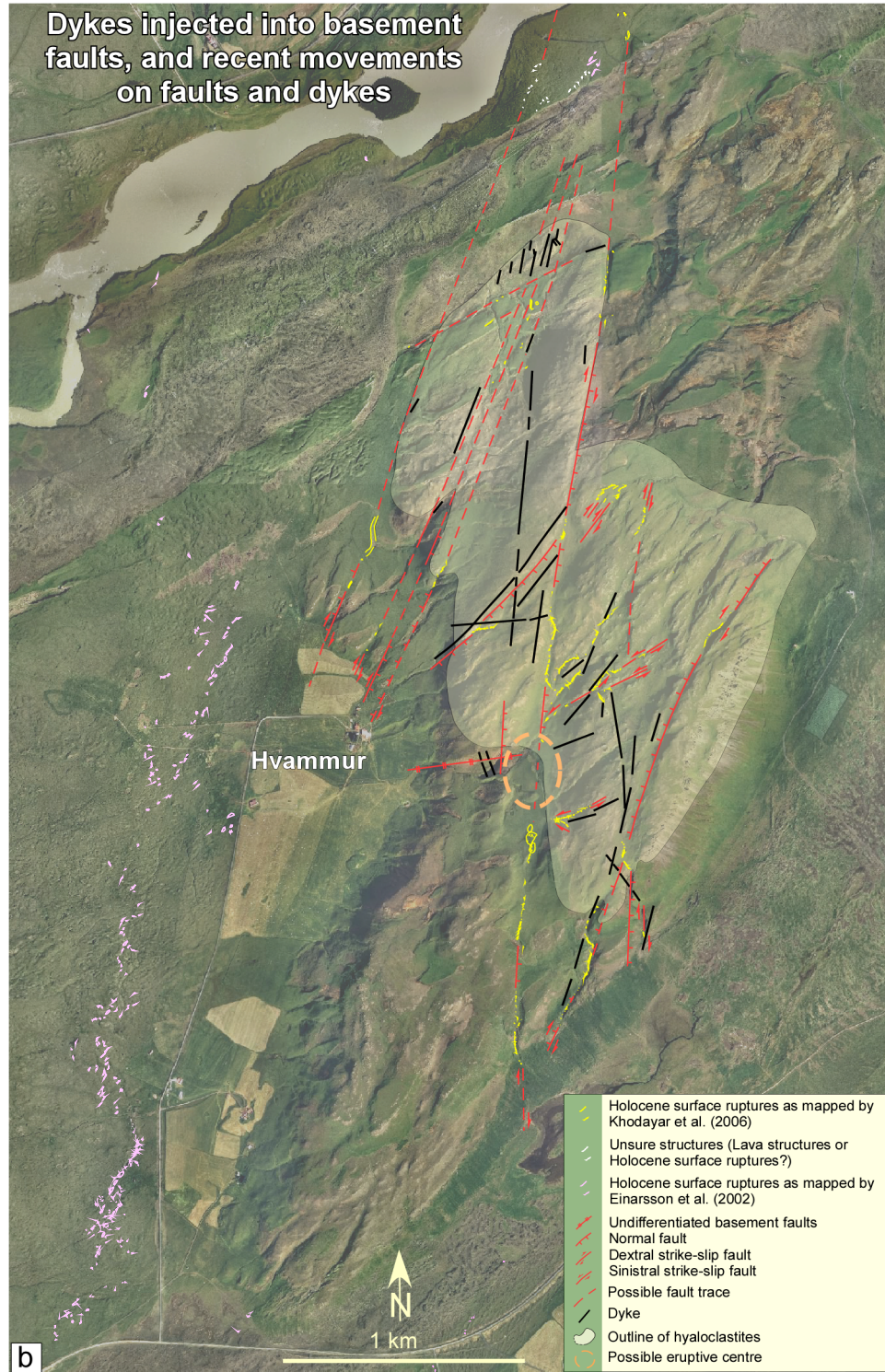


Tectonic Joints in Skarðsfjall

Refer to this map as:
 Maryam Khodayar, Hjalti Franzson, Páll Einarsson, and Sveinbjörn Björnsson
 Publication: ÍSOR-2007/017; LV-2007/065
 Based on field mapping in 2006



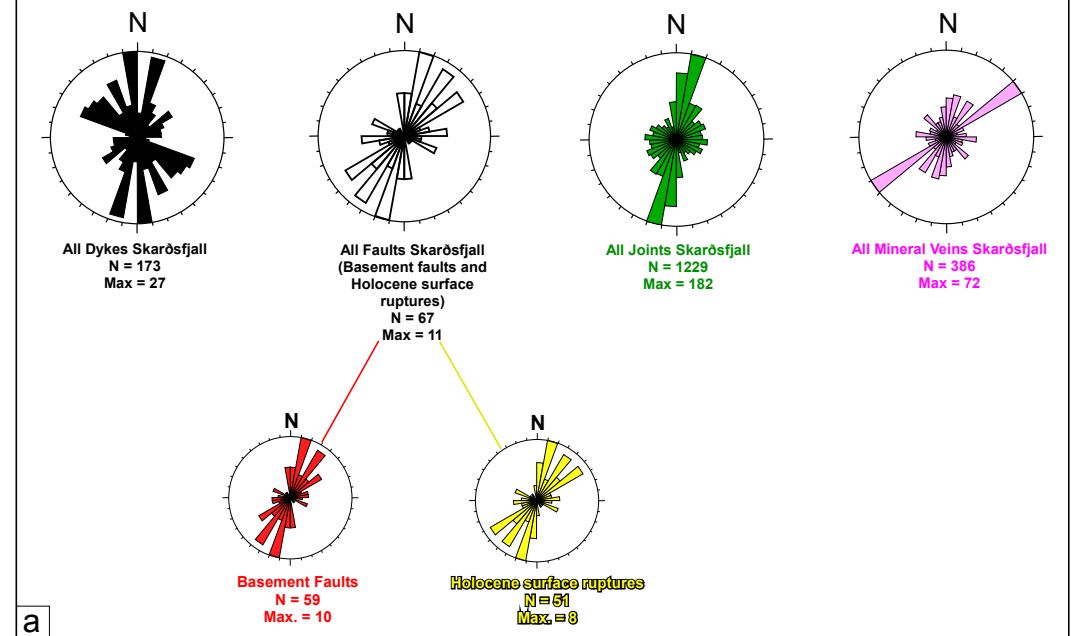
Dykes injected into basement faults, and recent movements on faults and dykes



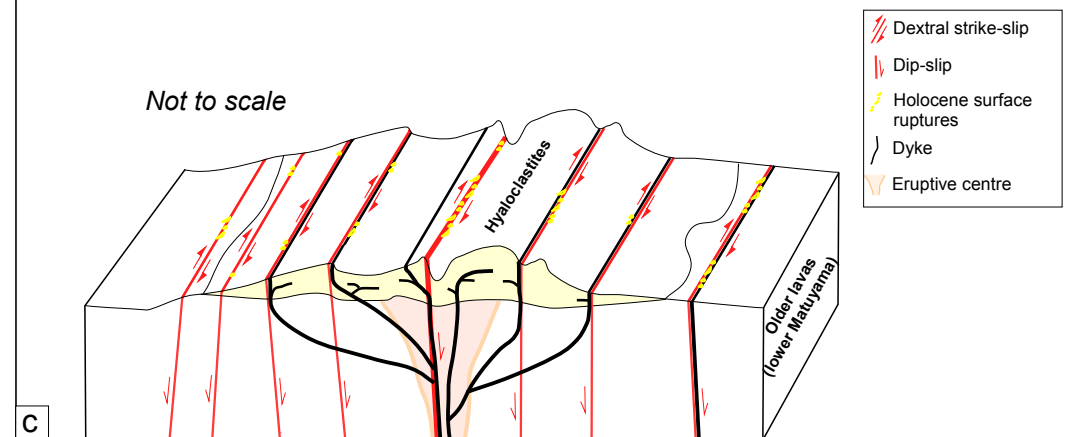
Fracture relationships in Skarösfjall

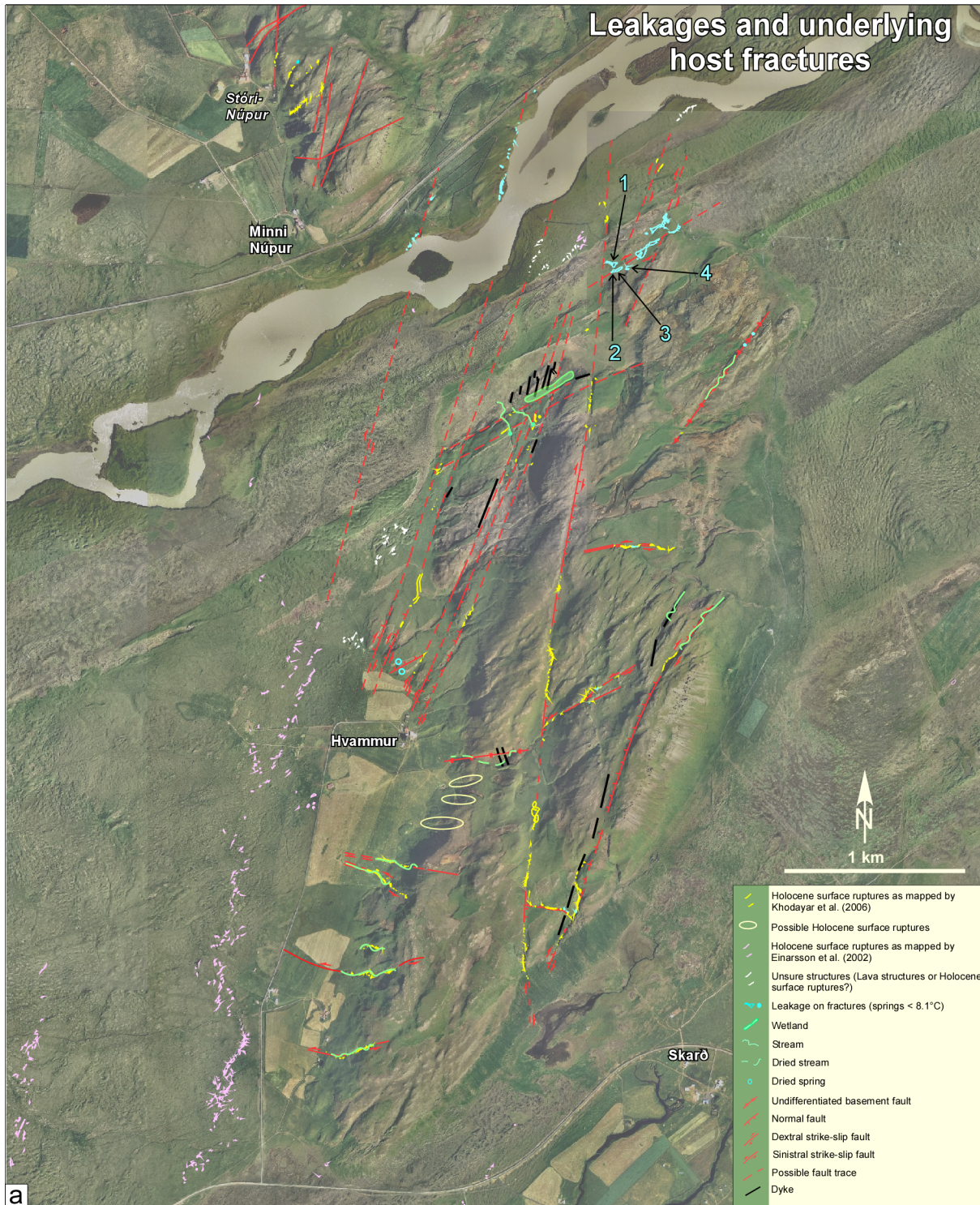
Refer to this map as:
 Maryam Khodayar, Hjalti Franzson, Páll Einarsson, and Sveinbjörn Björnsson
 Publication: ISOR-2007/017; LV-2007/065
 Based on field mapping in 2006

Strike-ranges of Dykes, Faults, Joints and Mineral Veins



Schematic cross-section of the relation between dykes, older faults, and Holocene movements along fractures

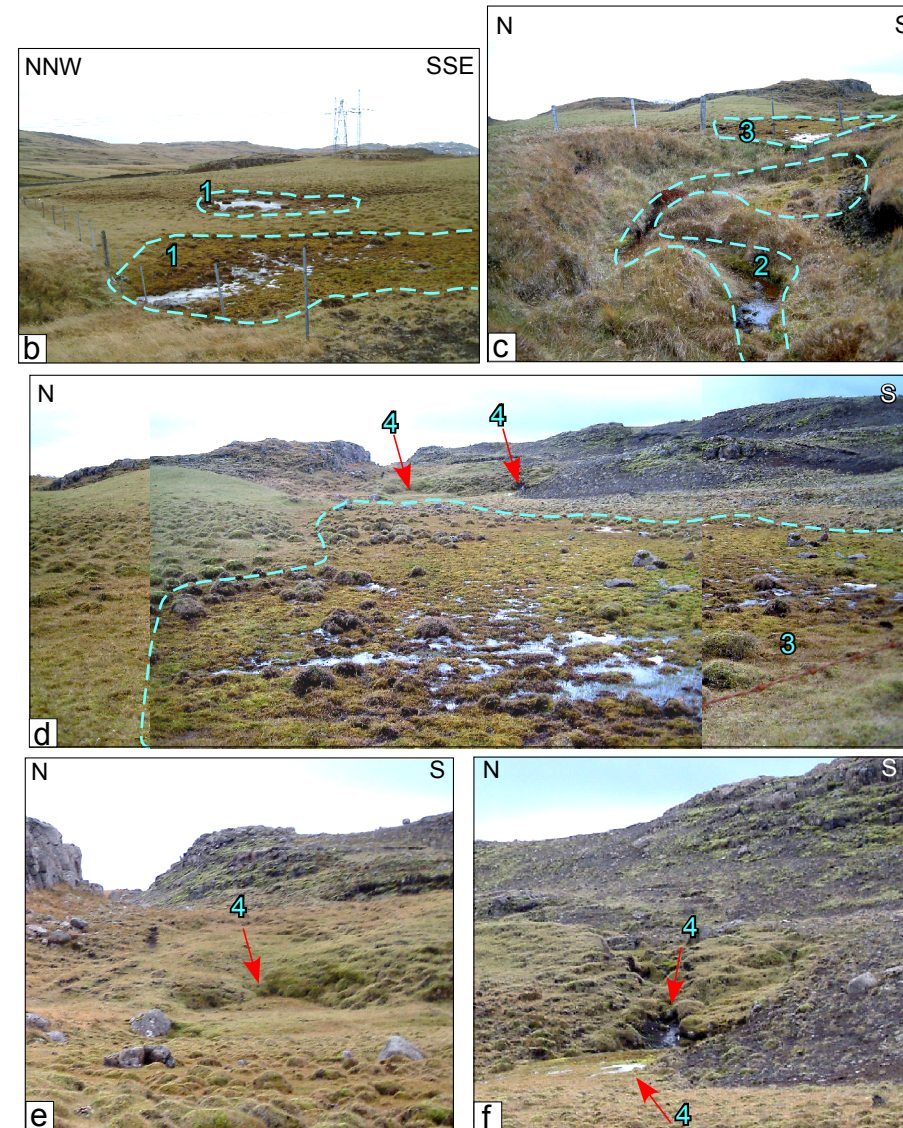




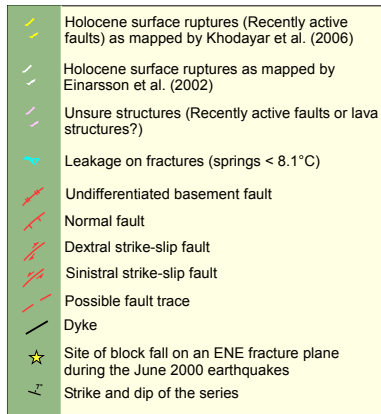
Faults, dykes, earthquake fractures and leakage

Refer to this map as:
Maryam Khodayar, Hjalti Franzson, Páll Einarsson, and Sveinbjörn Björnsson
Publication: ÍSOR-2007/017; LV-2007/065
Based on field mapping in 2006

Photographs of the leakages as numbered 1 to 4 on Map 7a



Correlation between the northerly fractures of Skarðsfjall and the Núpur area



Refer to this map as:
 Maryam Khodayar, Hjalti Franzson, Páll Einarsson, and Sveinbjörn Björnsson
 Publication: ÍSOR-2007/017; LV-2007/065
 Based on field mapping in 2006

Fractures mapped in Skarðsfjall are from Khodayar et al., 2007 (based on field mapping in 2006), and those in Núpur area are from Khodayar and Einarsson, 2002.

